UNIVERSIDAD CARLOS III DE MADRID

SCHOOL OF ENGINEERING

BIOENGINEERING AND AEROSPACE ENGINEERING DEPT.

BACHELOR THESIS

Biomedical Engineering

ROBUSTNESS AND ACCURACY EVALUATION OF A MULTICAMERA TRACKING SYSTEM

In collaboration with:

AUTHOR:	*ALONSO GARCÍA RUIZ*
TUTOR:	*EUGENIO MARINETTO CARRILLO*
DIRECTOR:	*JAVIER PASCAU GONZÁLEZ-GARZÓN*

September 2014

ACKNOWLEDGEMENTS

The years spent at university have been an unreplaceable experience. This thesis has thereafter a great symbolic meaning for me. It is my duty and my pleasure to deeply thank all the people that have made this possible and that have made it more approachable.

All my professors from the different specialities as well as the people in charge of the laboratories deserve a special mention for having listened to us all these years and building up a whole new degree. My colleagues and friends have become an essential component of my daily life, as well as my family, whose invaluable support will never flatten.

For their much appreciated assistance in this thesis, I must specially thank Henry, Laura and Iván from the BiiG and Santiago from Systems and Automatic Eng. Dept.. Ultimately, I would like to dedicate this project and send huge thanks to both my tutor Eugenio and my professor Javier for their motivation, their confidence in me and their patience.

ABSTRACT

Intra-Operative Electron Radiation Therapy (IOERT) consists on radiating the post-resected tumour bed or the unresected tumour during a surgery. This therapy is planned with the software *radiance*, developed from a collaborative work between Universidad Carlos III de Madrid (UC3M) and GMV (Madrid, Spain). The recently added tracking system (OptiTrack, NaturalPoint Inc., USA) allows for navigation and thus helps the clinician to follow the planning ([1]).

In order to study the dependence and the magnitude of the positioning error obtained with this tracking system, this project aims at comparing the positions given by the aforementioned camera system with those of an industrial robot that will act as a gold standard.

To achieve this, a Matlab client was developed to control the OptiTrack system by means of the Application Programming Interface provided and communicates with a RAPID robot server through a TCP/IP protocol, sending the positions and ordering the movements. A specific trajectory was designed in RobotStudio in order to cover the working volume in an operating room.

The results show the magnitude of the error of OptiTrack system and its spatial dependence, as well as the effect of different numbers of occluded cameras, different tracked tools and different calibration qualities.

This study will improve the new IOERT navigator using OptiTrack at HGGM by means of providing tracking error estimation during the procedure.

TABLE OF CONTENTS

1. INTRODUCTION

Image-guided interventions (or image-guided surgery, IGS) are medical procedures in which the position of surgical tools or therapeutic devices is displayed to the clinical expert regarding to preoperative imaging data, in order to facilitate decision making process. This approach has been followed in neurosurgery, orthopaedic, cardiovascular or radiation oncology applications, with the main purpose of improving performance, speed and security of procedures [2].

This section describes a brief introduction to Intra-Operative Electron Radiation Therapy (IOERT) and tracking as introduction of the actual setup at Hospital General Gregorio Marañón (HGGM).

1.1 IOERT

Radiation cancer treatments have evolved in the last fifty years mostly regarding the radiation distribution control over the cancerous and the surrounding healthy tissue [3].

Most tumours are treated with External Beam Radiation Therapy (EBRT) that delivers a high dose in the tumour volume by combining several irradiation fields from different orientations. There are also treatments like brachytherapy, where radioactive sources are directly placed near the target area during surgery or by using natural cavities.

Intra-Operative Radiation Therapy (IORT) consists of delivering a high dose directly to the tumour bed where the malignant cells are more exposed. This also makes it possible to protect or displace other tissues from the radiation, which provides a better survival rate [3]. IORT is sometimes combined with External Beam Radiation Therapy (EBRT) and chemotherapy ([3], [4]). Intra-Operative Electron Radiation Therapy (IOERT) takes advantage of electron radiation, as its dose falls down rapidly after interacting with the target tissue [4].

Japanese researchers started using similar IORT methods to the current ones in the 1960s followed by the US in the 1970s and Europe in the 1980s. Its use has continued to spread and improve during the following decades, both for IOERT and high-dose rate brachytherapy (HDR-IORT) treatments [3].

Figure 1 from [1]
IOERT applicator.

For IOERT the radiation is applied to an area with a rigid cylinder (called applicator, Figure 1). Once the applicator is placed over the treatment area, it is attached to a linear accelerator (Figure 2) in order to deliver the dose. Specific mobile linear accelerators are available, which are moved to the OR before the procedure and moved back after treatment.

Figure 2
Mobile accelerator unit.

The local control of the tumour cells depends on the dose, which mainly increases with tumour stage and on tumour volume [3]. The successfulness of the treatment will therefore depend on the correct delivering of the dose.

Through IOERT, the radiation oncologist must estimate the delivered dose and the area to be radiated with the help of the surgeon. For that, he must also choose the applicator size and bevel, its depth and its position. This estimation will mainly be based on previous procedures and on his experience.

Hence, it may be of use if those results and experience obtained from IOERT so far would be collected together, studied and shown to the physicians specifically for each case. Also, there was the need for a reference to plan a treatment in advance.

The IOERT planning software *radiance* (GMV, Madrid, Spain) provides a reference close to the real-case scenario, taking into account all the

parameters and factors that affect the dose and making possible the pre-, intra- and post- planning simulations [5]. This planning software was initially proposed by the BiiG (Biomedical Imaging and Instrumentation Group) in HGGM and is now available as a commercial product developed by GMV ([5], [6]).

The Treatment Planning System *radiance* loads 3D images (CT scans) and shows orthogonal 2D and reconstructed 3D visualization. This software allows the user to perform segmentation of organs. Based on Hounsfield Units provided by CT images, it performs a simulation (Figure 3) of the electron beam radiation applied by a virtual applicator (IOERT) through different tissues, depending on the energy, the bevel angle and the depth and shows the dose-to-volume curves for every affected organ (Figure 3, [5]).
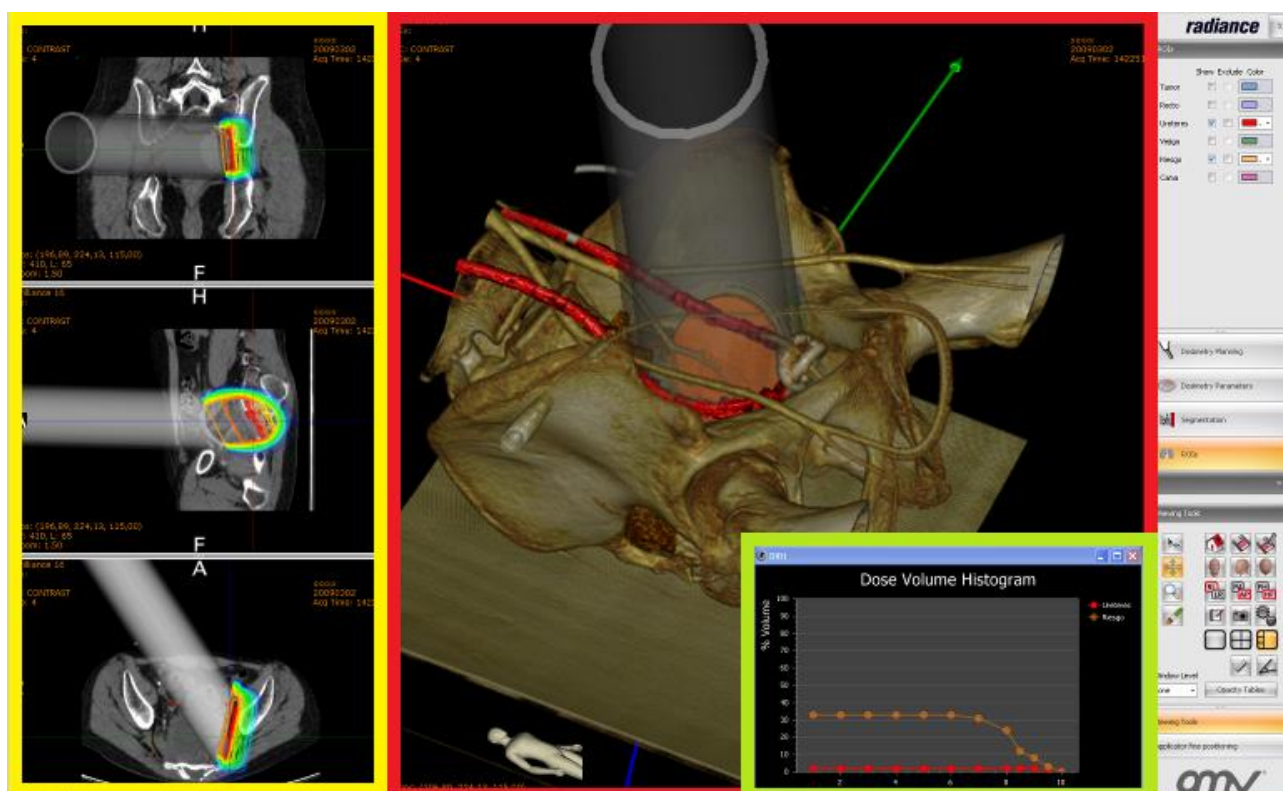

Figure 3 from [7]
Capture from radiance: 3D reconstruction (red), representation of the dosage over the area in 2D images (yellow) and the dose-to-volume histogram (green).

This software is currently under clinical trials by the BiiG in the HGGM among other hospitals. This study belongs to the same HGGM research project on IOERT and *radiance*.

1.2 TRACKING SYSTEMS

A tracking system is a device that follows the position of objects in real-time. It gives the spatial location of an element in the operating room (OR). This serves the IGS navigator to locate the instruments in the images relative to the patient's anatomy during a medical procedure. In other words, to relate the OR geometric space with the image space, finding the geometric translation between them (Figure 4).

Since they correspond one to the other, now the images not only show the anatomy, relevant structures or function but serve as a guiding live map to the physician ([8]) during the procedure. This makes possible real-time procedure plannings. Thus, clinicians can obtain additional information for the procedure.
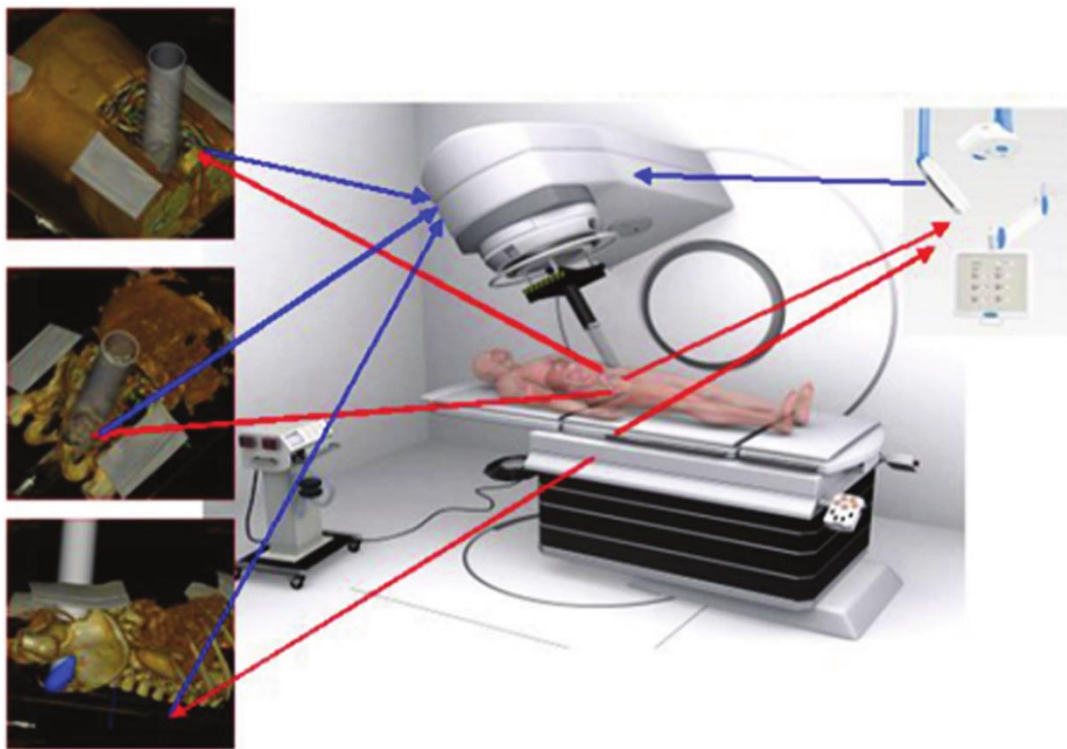

Figure 4 from [9]
Simulation of an IOERT procedure with radiance. In the upper right corner there is an example of a tracking system. The arrows show the relation between the virtual and real applicators.

A navigation system has been recently integrated in *radiance* Treatment Planning System providing real-time tracking during the procedure. Though it is fully functional and already available in the OR, it is under development at the HGGM by the BiiG.

Following the planning correctly depends on the navigation. The procedure is helped with the positioning of the applicator along the patient's anatomy using the previous CT scan.

1.2.1 OPTITRACK OPTICAL TRACKING SYSTEM

Tracking has evolved from stereotactic frames meant for neurosurgery (Figure 5) to tracked markers for almost any surgical procedure, due to the integration of CT and MRI scans in the last decades [10].
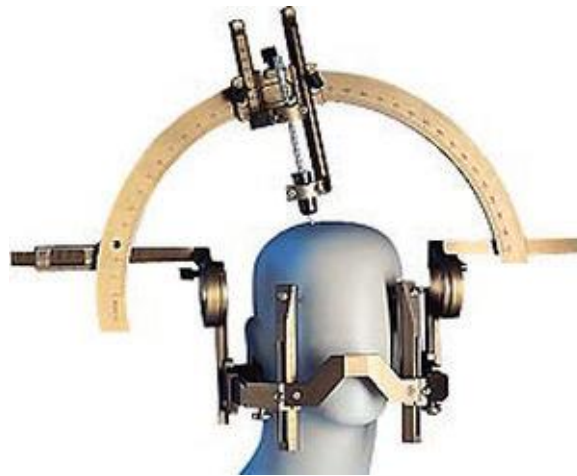
Figure 5 from [11]
Stereotactic frame (mechanical tracking) for neurosurgery.

Among the available tracking technology (mechanical, electromagnetic and optical), optical systems show high precision and the greatest tracked area [10], [12]. As a drawback, they need a clean line-of-sight of the tracked object, which is not possible within the body, i.e. with catheters or probes, for which electromagnetic ones are more indicated. Depending on the application, the area and the accuracy required, one or another system may be chosen [10].

At HGGM, image-guided IOERT equipment uses the optical system OptiTrack (NaturalPoint Inc., OR, USA). This system can handle up to ninety six cameras.

As several cameras may be occluded during an operation and the covered volume is high, the HGGM OR consists of eight cameras model OptiTrack Flex 13 ([13], Figure 6).

Each of these has 28 near-infrared (IR, 850nm) light-emitting diodes (LED) with 1280x1024 pixels image size and up to 120 frames per second

(fps). They detect the objects that reflect IR light (800nm long pass filter), filtering the rest of the spectrum [13]. The tracked objects, called rigid-body tools (Figure 8), have special IR-reflective balls, called markers (Figure 8), so that they are detected by the cameras.

This tracking system meets the characteristics for IOERT application, because the applicator is an external, non-flexible object that will stay static once positioned and it covers the needed working area.

Figure 6 from [13]
NaturalPoint OptiTrack Flex 13 camera

These cameras are arranged around the area where tracking is needed (Figure 13).

The system calculates the position of the passive retro-reflective markers (Figure 8). As mentioned, these are small balls (1 cm) coated with IR-reflective material. The position is obtained in real-time by a forward projection approach ([14]). Each marker is located at the intersection of the projected rays of every camera (Figure 7).
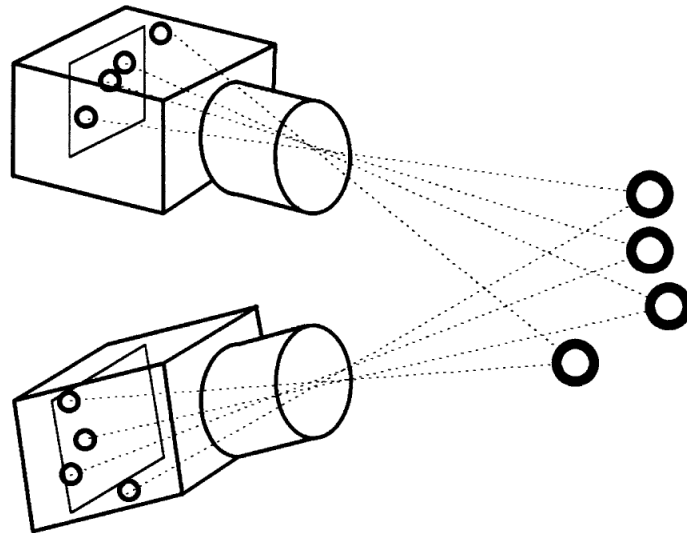
Figure 7 from [15]
"Two cameras imaging four retro-reflective targets. Target locations are determined from a forward projection of the target images on the camera image plane. Targets lie at the intersection of the projected rays" (R. Gooch, 1998, [15]*).*

On a rigid-body tool (Figure 8, right), the reflective markers are positioned in a unique geometry (i.e. they form an unmistakable shape for any orientation) that is identified by the cameras, allowing them to locate the tool in position and orientation (6 DOF). To identify a rigid tool it must have at least three markers with static distances and angles between them ([12]).

The pointer at the right of Figure 8 is a tool designed by the BiiG (Biomedical Imaging and Instrumentation Group) at HGGM ([12]) that includes six reflective markers. Another rigid-body tool is attached to the applicator (Figure 23) and thus the position and orientation of the applicator can be now inferred from the tracked markers.

Figure 8
Left: set of retro-reflective markers.
Right: rigid-body tool with markers.

OptiTrack cameras must be calibrated for the system to know the position of each camera in the space. Once the tracking system is calibrated, the IGS navigation system is able to show the tools throughout the patient images.

In IOERT, the main element to be tracked is the applicator (Figure 1). The configuration for the virtual applicator in the planning includes the position, depth and bevel angle. It can be compared then to the applicator configuration over the patient, allowing the clinician to check the desired positioning according to the plan.

Compared to other tracking systems, OptiTrack has great flexibility in configuration, yet the need for calibrations. However, its use is not spread for medical applications. One of the main tracking brands developing medical solutions is Northern Digital Inc. (NDI, USA), which produces the Polaris optical tracking systems (Figure 9, [16]).

These devices consist of two cameras separated by a known fixed distance. Besides the implicit limitation on the tracked volume, which is smaller than Optitrack's, and the accuracy, it ensures having always the same coverage with the same expected error distribution (Figure 10).

Although several NDI devices employed together may cover a greater space, they do not share the information between them, while OptiTrack does. In this respect, OptiTrack has greater potential with support for ninety six cameras at desired distance but at the same time the risks of disturbing the system (i.e. moving a camera) and the inconvenience of performing calibrations.

Figure 9 from [16]
NDI Polaris Spectra (big) and Vicra (small).
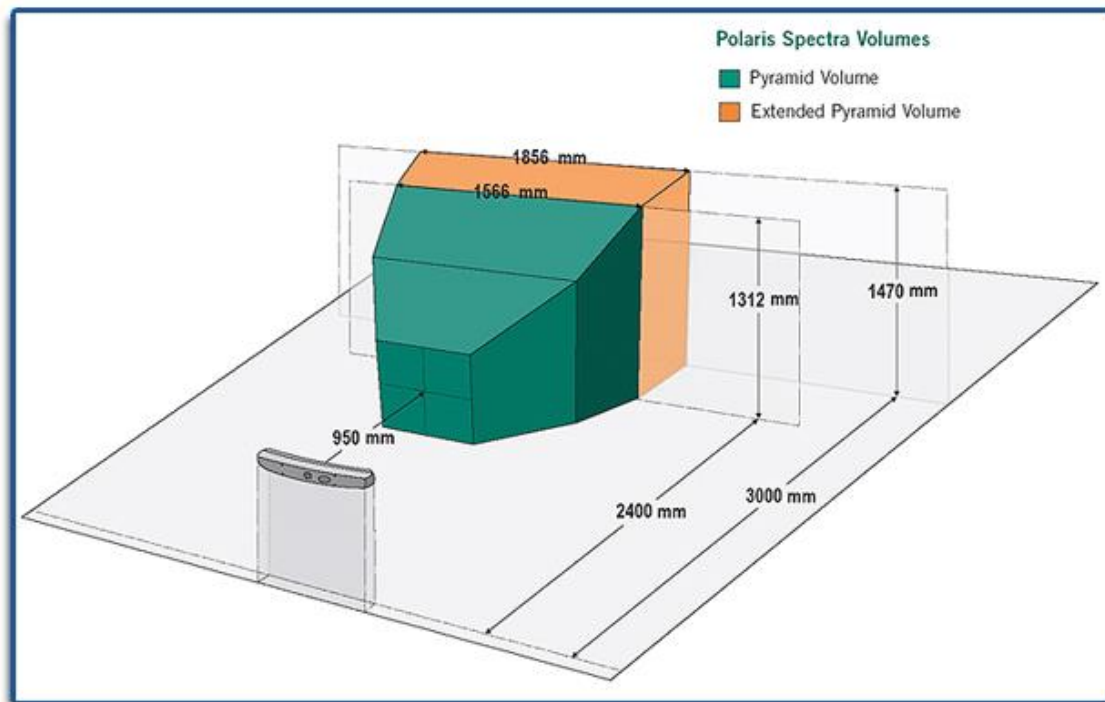
Figure 10 from [16]
NDI Polaris Spectra covered volume

Before this study, a previous analysis of OptiTrack system was made by the BiiG at the HGGM ([12]). As it will be described, the accuracy of the pointer tip was estimated with respect to a millimetre board, which introduces additional error sources.

2. MOTIVATION AND OBJECTIVES

Regarding the tracking system, occluded cameras and different elements like markers size, the tool geometry and the calibration can also affect its performance in different ways and, more importantly, the physician may not be aware of it ([17]), so the study of these factors is also of interest. Ultimately, the study of the strengths and limitations of the tracking system could give the physicians an idea of the accuracy to be expected in real-time in a surgery.

One attempt to estimate the error in the pointer tip (*pivot* of the rigid-body tool) was made by the BiiG at the HGGM ([12]) under the same overall project. This was performed placing the pointer on seventeen different locations on a millimetre board (Figure 11).

The results yielded 1.7mm ± 0.5mm (RMS ± standard deviation) at the centre and 2.2mm ± 0.2mm at one meter distance.
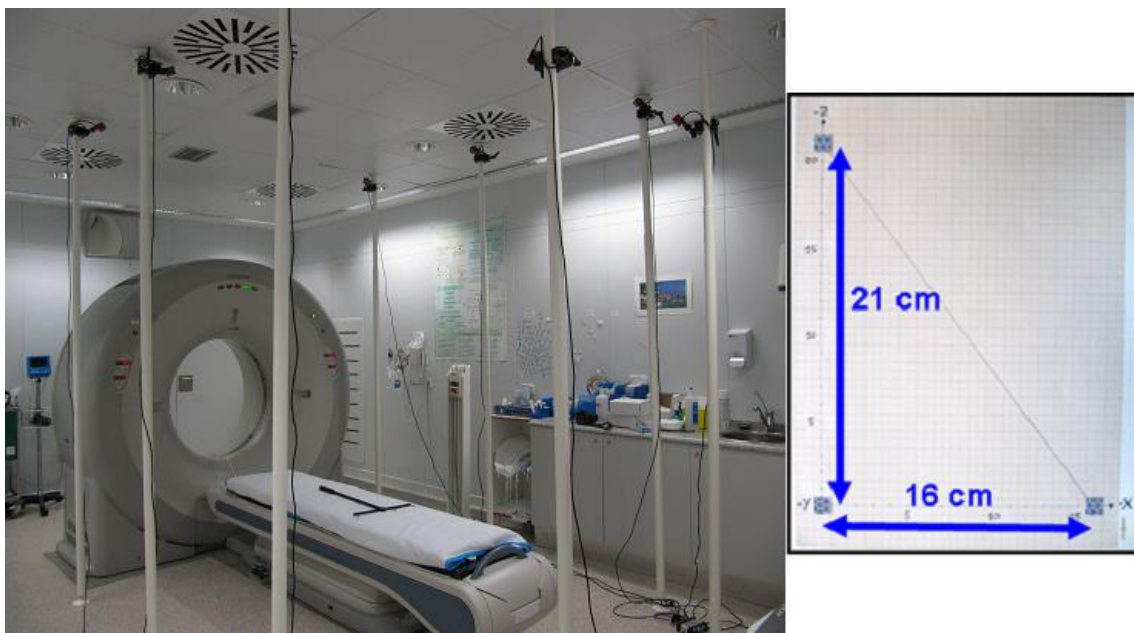

Figure 11 from [1]
Left: OptiTrack tracking camera system installed at the CT room.
Right: millimetre board.

This try-out was meant to have an estimated measure of the error of the pointer pivot in several spatial locations. However, it was susceptible to other error sources like the human eye perception, a steady hand or the precision of the millimetre board that were not quantified.

Also, different factors that can affect the outcome are still unknown, like the type of tool or the number of operative cameras. A possible approach to solve this problem is isolating and measuring each of the error sources individually.

Apart from this trial, there is no other study that has published other accuracy evaluation of this tracking system thus far. The OptiTrack official documentation also lacks information about the mathematical methods used by the cameras to calculate errors, so there is no precise insight of the system error once the calibration is performed.

Since OptiTrack is the system used for the IOERT navigation at the HGGM, a deep tracking accuracy study is needed in order to characterize the spatial error distribution.

The OptiTrack system calculates the position of a rigid-body tool by means of a least-squares approximation from all the tool's markers. However, this masks the error in one individual marker. An appropriate approach would be to measure the position of one only marker to isolate Optitrack error source from this approximation error.

It is also important to know how several real-life factors influence on it, such as the performed calibration, the tool used and the number of occluded cameras. A thorough study could help providing a more realistic assistance during the surgical procedure.

The objective of this project is to evaluate the absolute accuracy of the optical tracking system OptiTrack, specifically for its application in the IOERT at HGGM employing an ABB robotic arm (Figure 17) as gold standard: its repeatability error of 0.02mm ([18]) is considered at least one order of magnitude below from the camera error.

The results will determine valuable information not only for the implemented IOERT system of the HGGM, but more generally to present the limitations of the current OptiTrack system to any other application that makes use of it, as nobody has done it before.

2.1   PLANNING

The project was introduced on January 2014 and it extends till September 2014, lasting about nine months. A summary of the plan is represented in Table 1.

After the initial documentation and basic knowledge of C++ language, it followed the first steps using OptiTrack and the API. The first

tracking measurements and figures were obtained using the engineering software Matlab.

Then a dummy server simulating the robot was implemented in order to learn the TCP/IP principles and usage. After that, the server code (written in RAPID language) and the communication between client and server were developed using a virtual robot controller in the software RobotStudio.

With the same software, the trajectories of the robot were designed and tested before implementing it in the actual robot.

Once the environment was complete with all the cameras installed around the robot, the acquisitions started and the data was saved for analysis. After the analysis, the results and conclusions are written and shown in this thesis.
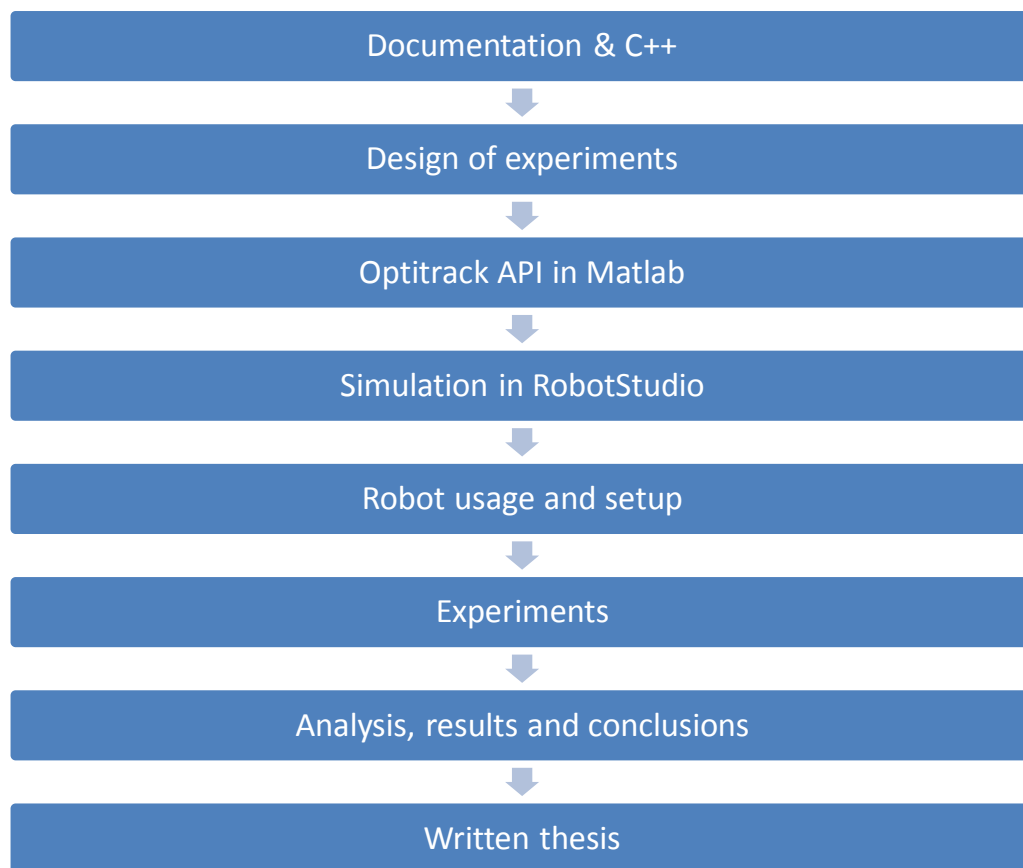
| Documentation & C++ |
| Design of experiments |
| Optitrack API in Matlab |
| Simulation in RobotStudio |
| Robot usage and setup |
| Experiments |
| Analysis, results and conclusions |
| Written thesis |

Table 1
Project planning

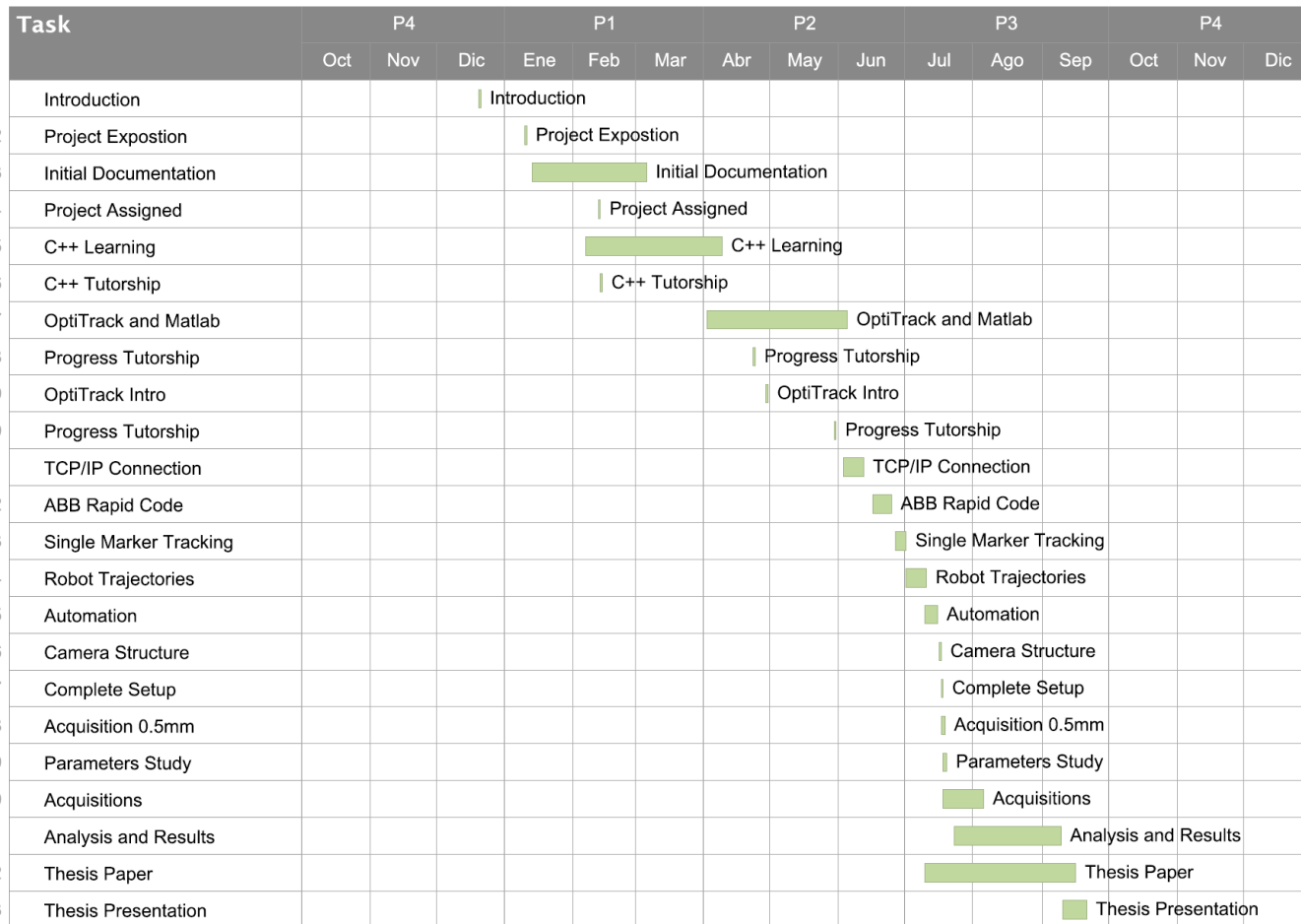The Gantt chart shows the progress of the different steps over time:

Task	P4			P1			P2			P3			P4		
	Oct	Nov	Dic	Ene	Feb	Mar	Abr	May	Jun	Jul	Ago	Sep	Oct	Nov	Dic
1 Introduction				Introduction											
2 Project Expostion					Project Expostion										
3 Initial Documentation				Initial Documentation											
4 Project Assigned					Project Assigned										
5 C++ Learning					C++ Learning										
6 C++ Tutorship					C++ Tutorship										
7 OptiTrack and Matlab							OptiTrack and Matlab								
8 Progress Tutorship							Progress Tutorship								
9 OptiTrack Intro							OptiTrack Intro								
10 Progress Tutorship								Progress Tutorship							
11 TCP/IP Connection								TCP/IP Connection							
12 ABB Rapid Code								ABB Rapid Code							
13 Single Marker Tracking								Single Marker Tracking							
14 Robot Trajectories								Robot Trajectories							
15 Automation								Automation							
16 Camera Structure									Camera Structure						
17 Complete Setup									Complete Setup						
18 Acquisition 0.5mm									Acquisition 0.5mm						
19 Parameters Study									Parameters Study						
20 Acquisitions									Acquisitions						
21 Analysis and Results										Analysis and Results					
22 Thesis Paper										Thesis Paper					
23 Thesis Presentation												Thesis Presentation			

Figure 12
Gantt chart of the project.

2.2 COST PROJECTION

The estimated costs of this project come from the human resources (Bachelor coordinator and student) and from the equipment used.

Participants	Salary (€/hour)	Hours	Total cost
Project coordinator	35.00	480	16800
Bachelor Student	25.00	542	13550

Table 2
Human resources costs.

The costs of using each material are calculated based on its depreciation in time and the total time of usage. There are elements for which the depreciation is unknown, and thus its lifespan is considered to be the duration of the project.

For instance, a 1000 euros PC has an average lifespan of 5 years, then its depreciation is 1000 euros / 5 years = 200 euros/year, and after 5 years its value is zero.

Equipment	Unit Cost (€)	Units	Lifespan (months)	Depreciation per Month (€/month)	Months employed	Total Cost (€)
Camera Flex 13	746,25	8	24	31.09	9	2238.76
OptiHub 2	223,35	2	24	9.31	9	167.51
Camera Clamps	62,75	8	24	2.61	9	188.24
OptiWand kit	186,00	1	24	7.75	9	69.75
Hardware Key	73,95	1	24	3.08	9	27.73
USB camera cable	7,47	8	24	0.31	9	22.41
USB hub cable	3,74	2	24	0.16	9	2.80
Tracking Tools	746,25	1	12	62.19	9	559.69
Cage structure	700,00	1	9	77.78	9	700.00
Robot ABB 1600	22050,00	1	144	153.13	2	306.25
Matlab	500,00	1	12	41.67	9	375.00
MS Office 2010	139,00	1	24	5.79	9	52.13
RobotStudio	380	1	12	31.67	5	158.33
PC	1000,00	1	60	16.67	9	150.00
						5018.61

Table 3
Equipment costs.

All the prices listed for OptiTrack products (from cameras to Tracking Tools) are taken from the NaturalPoint Inc. website ([19]). The prices appear in USD and they have been converted to Euros by the currency exchange: 0.747 €/USD. The price for the ABB robot has been taken from [20] and converted from Irish pounds by 1.26 €/pound, while its lifespan is estimated in [21]. The software prices and depreciations are the ones corresponding to licenses and its period of time.

The final estimation is:

Project Parts	Cost (€)
Human resources	30350.00
Equipment	5018.61
	35368.61

Table 4
Total costs.

3. MATERIALS

3.1 LIST OF MATERIALS

Here it is a summary of the materials needed to develop the project:

Tracking system

- 8 OptiTrack Flex 13 cameras
- 8 Manfrotto Super Clamps
- 8 USB camera cables
- 2 USB hub cables
- 2 USB hubs
- 1 hardware USB key
- Tracking Tools software license
- BiiG, Polaris (NDI), applicator and star-shaped rigid bodies
- OptiWand kit (Calibration wand)

Engineering software Mathworks Matlab R2012a

- MS VS C++ compiler (2010) (MS Win SDK 7.1)

Robot simulation software ABB RobotStudio 5.60 with RobotWare

Robot ABB IRB 1600

Custom tool clamp for robot

Cage structure

Personal computer

MS Office 2010

Table 5
List of materials.

3.2 TRACKING SYSTEM

To mimic the system set up at HGGM (Figure 13 and 1.2.1) eight OptiTrack cameras were needed, as well as a mounted structure and the clamps to hold the cameras (Figure 21, Figure 14). The HGGM setup size

was measured and replicated so that the robot takes the place of the surgeon and moves along a simulated operating room.
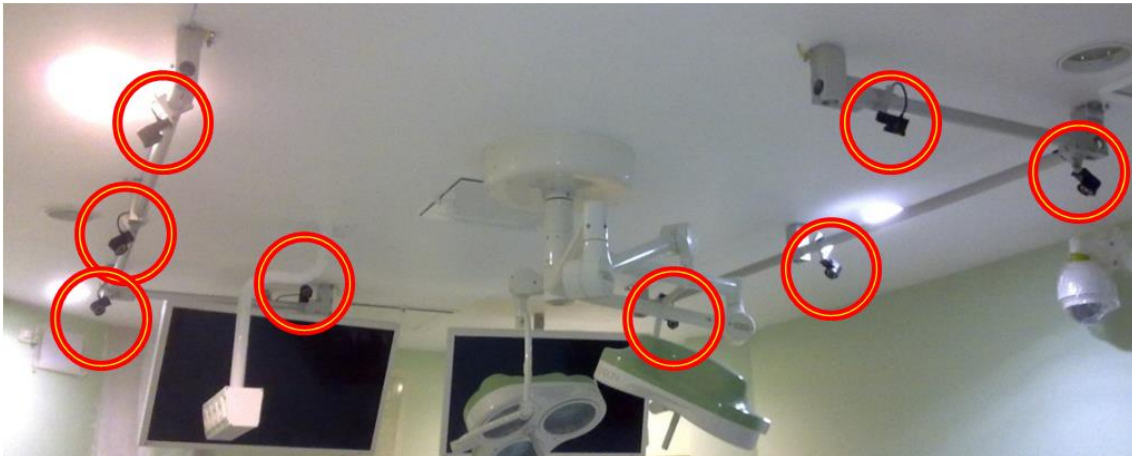
Figure 13
HGGM OR camera setup.

Figure 14
From left to right: camera clamp, camera-to-clamp connector and camera.

The cameras are connected to a PC through two USB hubs (Figure 15).

Figure 15
OptiTrack OptiHub-2 USB hub

The software Tracking Tools (NaturalPoint Inc., OR, USA, [22]) controls and calibrates the OptiTrack cameras. Before tracking, it is needed to verify the license, focus the cameras correctly, calibrate them, display and correct for undesired reflections.

A marker tool specifically designed to calibrate the cameras is also needed (*OptiWand*, Figure 16).

Figure 16
OptiWand, a tool used to calibrate the cameras.

The system takes the position information of every individual marker, each with an unknown location error, to calculate and fit an approximated position for the centroid of the rigid body (or *trackable*), using a least-squares approximation. This location can then be translated to another point, called *pivot*, which is usually the tip of the tool.

The different tracking functions are controlled through the OptiTrack Tracking Tools API, which is loaded in Matlab for this project. Matlab is multipurpose engineering software from Mathworks whose main characteristic is that it can work with matrix-form variables. The API is an interface to the system which allows Matlab to collect positions of a rigid body's pivot and also from markers on a marker cloud.

3.3   ABB ROBOT

The robot used is an industrial ABB IRB 1600 with 1.2 m of reachability and 6 kg of maximum load at the tip. This robot has a position repeatability error of 0.02 mm [18], an accuracy that is expected to be at least one order of magnitude better from that of the optical tracking system.
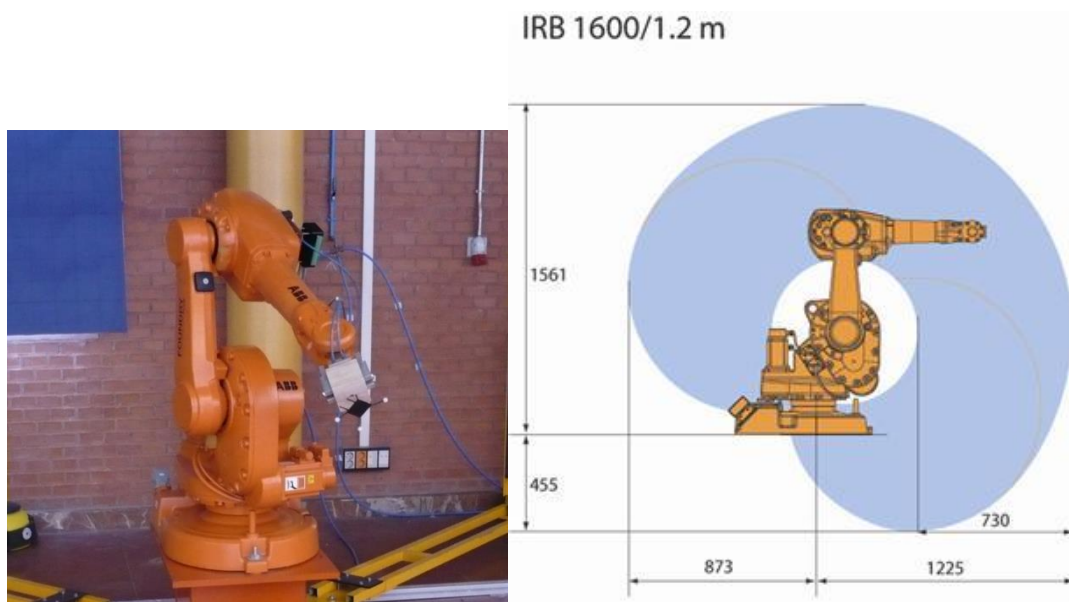
Figure 17, right image from [18]
Robot ABB IRB 1600.

The robot has a hand-held device of the controller using MS Windows operating system, called FlexPendant (Figure 19). From this device, the robot can be moved manually or automatically if the code is loaded. The Play and Stop buttons on the Flexpendant let run or stop the running code.

To select the work mode of the robot, there is a key in the controller box (Figure 18) that allows Automatic, Manual and Manual 100% modes. In Manual modes, the user must be pressing the safety pressure button at the FlexPendant during all the robot activity.

The robot also has a service port (Figure 18) on the controller box to connect to the computer through an Ethernet cable.
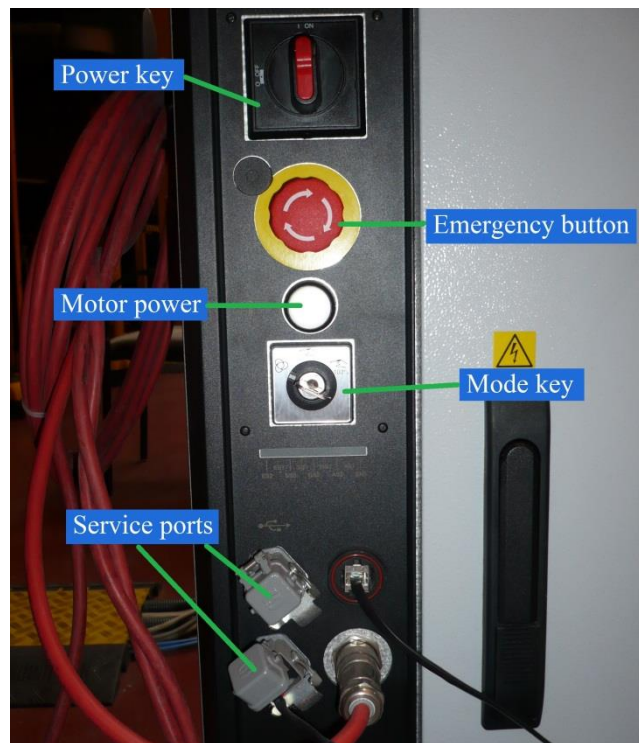
Figure 18
Panel of the controller box of the ABB robot.
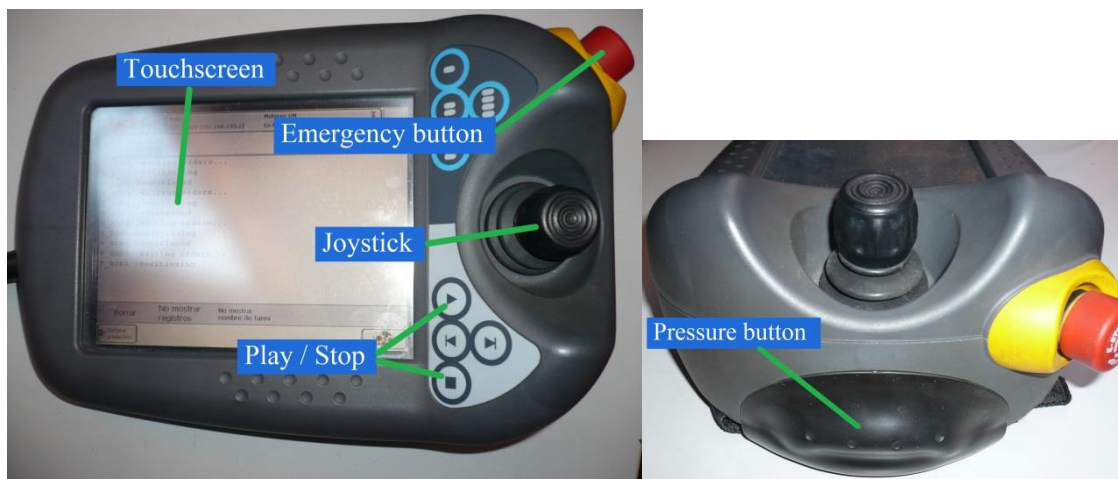
Figure 19
FlexPendant, a hand-held device of the robot controller.

3.4 EXPERIMENTAL SETUP

With a metallic structure built around it, the robot is surrounded by the OptiTrack cameras (Figure 21) simulating the operating room set up (Figure 13).
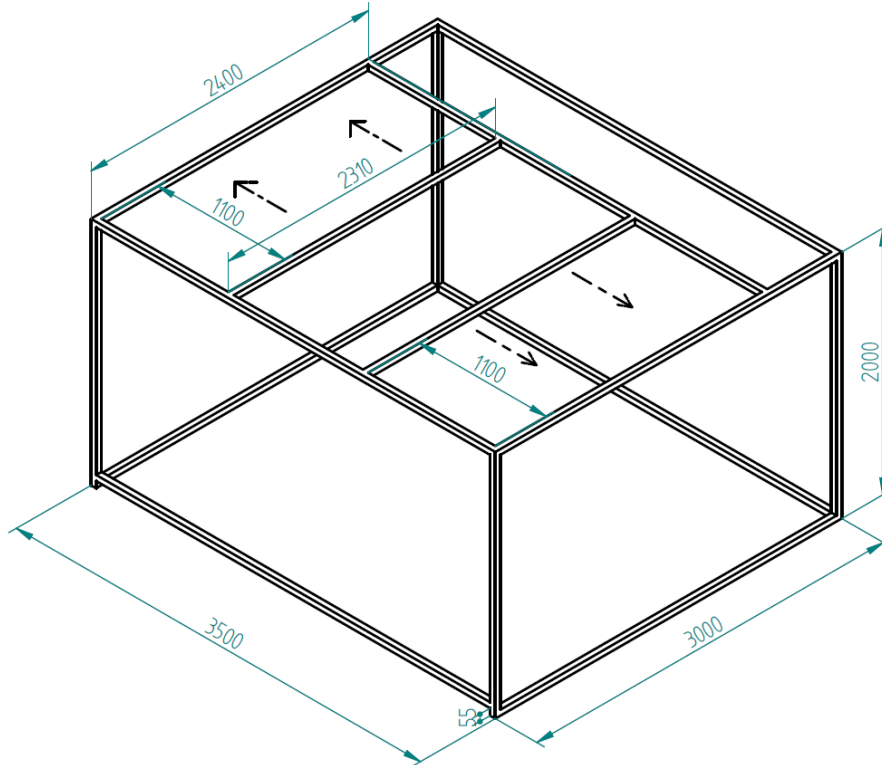
Figure 20
Metallic structure diagram.
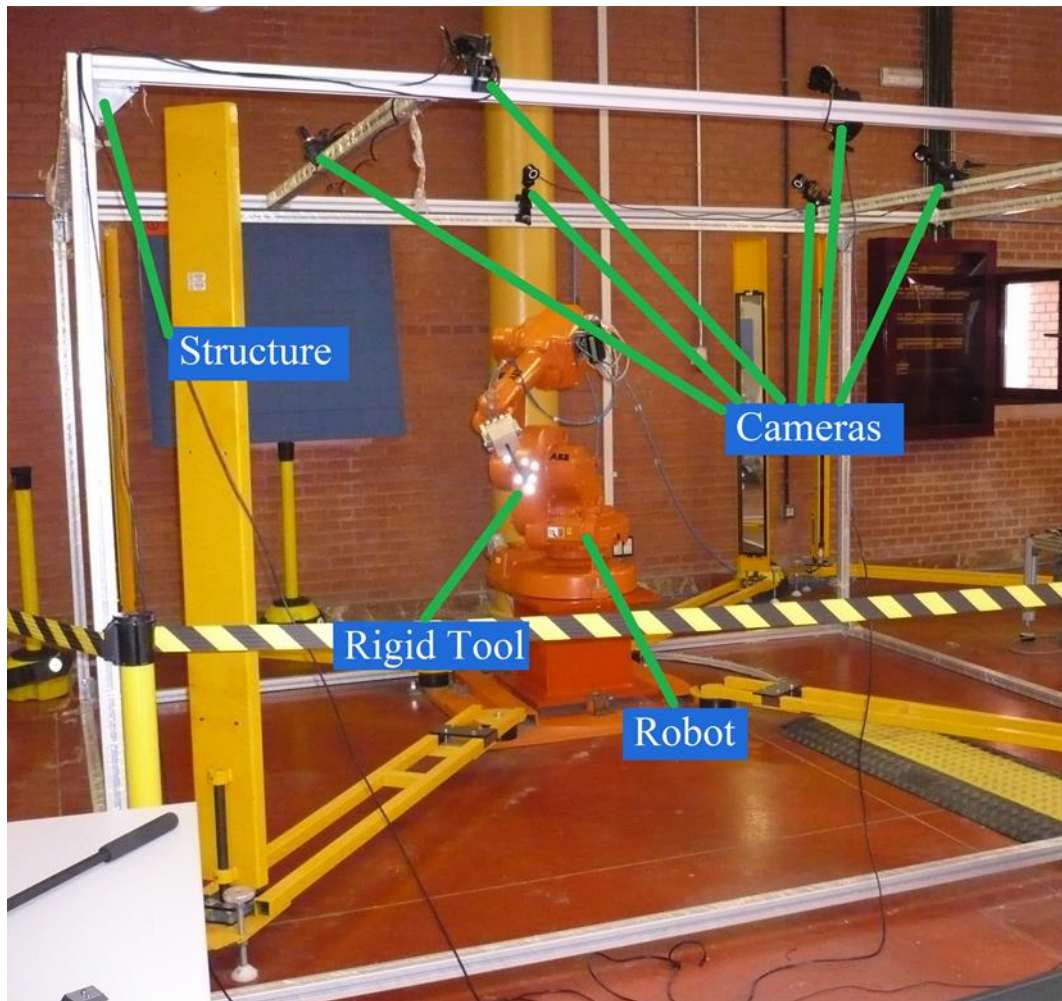
Figure 21
ABB Robot inside the cage structure that holds the cameras.
The pointer tool is attached to the robot by a custom clamp.

The robot has a custom clamp (Figure 22) that permits the attachment of the rigid-body tools in Figure 23. This clamp was specially designed in-house in order to fit the employed tools.

Figure 22
Custom robot clamp to attach rigid-body tools.

Figure 23
Several tools, from left to right: BiiG, Polaris, rigid-body and applicator pointers.

On a computer, the software Matlab, Tracking Tools and RobotStudio are used.

RobotStudio is a program from the robot company ABB that performs robot simulations. It loads 3D environments and makes possible to create robot paths and RAPID scripts, as well as connecting to the actual robot controller.

4. METHODS

This section describes first the hardware and software interconnection in order to carry out the experiments and data acquisition. Data is collected using a computer where a controller software is running. The robot is ordered to move through a predefined path using this software. Then the position data from the tracker is acquired and saved into a file. This process is repeated for each position along the path.

A server code was coded in RAPID language for this project in order to control the movement of the robot. This software was simulated using RobotStudio previously. In order to run the server, code must be loaded into FlexPendant (Figure 19).

Robot connects to the computer through an Ethernet interface provided by FlexPendant and using the server application (Figure 18) on the controller box.

Once server is connected to the robot, a client application (also coded for the project) is connected to the server using a socket link and the Ethernet interface. Client is run on Matlab software. In order to move it through the predefined path, the client sends the positions to the robot. The robot moves an attached rigid-body under the OptiTrack cameras field of view. The robot server communicates when the robot is positioned to the client and for each point, the tracker provides the position of the tool. Then this position and the robot point are saved in a file for further analysis.

4.1   CALIBRATION OF THE CAMERAS

As commented, these cameras must be calibrated so the system correctly locates tools in 3D-space. The fairness of the calibration performed is user-dependent and will affect the error of the tracking information. Thus it is important to follow a protocol that ensures good calibration results and repeatability. The same procedure, used by the BiiG at the HGGM, was replicated for the calibration of the system in this project.

The main system calibration steps are listed here:

```
┌─────────────────────────────────────────┐
│      Position and focus the cameras      │
└─────────────────────────────────────────┘
                    ▼
┌─────────────────────────────────────────┐
│            Correct for reflections       │
└─────────────────────────────────────────┘
                    ▼
┌─────────────────────────────────────────┐
│               Pre-calibration            │
└─────────────────────────────────────────┘
                    ▼
┌─────────────────────────────────────────┐
│            Second pre-calibration        │
└─────────────────────────────────────────┘
                    ▼
┌─────────────────────────────────────────┐
│               Final calibration          │
└─────────────────────────────────────────┘
                    ▼
┌─────────────────────────────────────────┐
│             Save calibration file        │
└─────────────────────────────────────────┘
```
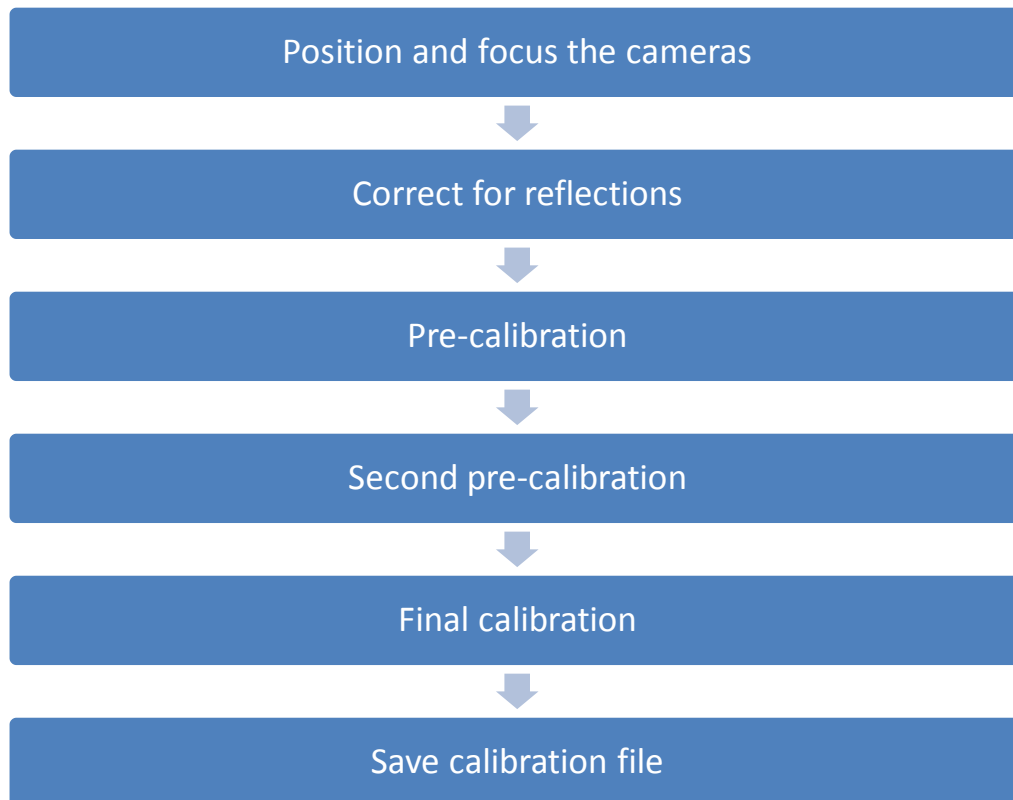
Table 6
Calibration steps.

First, cameras are placed and focused towards the area of interest. During calibration, the cameras are checked in order to keep the line-of-sight to the tracked volume. All reflective material items must be moved away before running the calibration software.

Once tracking volume is ready, the *Optiwand* tool (Figure 16) is used to perform the calibration using the Tracking Tools software. This tool is moved smoothly through the focused volume of the cameras during the calibration. Tracking Tools collects pose information from the cameras and *Optiwand* and performs an iterative process to estimate the calibration parameters of the system. In order to obtain a maximum quality calibration, this step is repeated three times (Pre, Second and Final in Table 6). Each iterative process starts from the solution of the previous one until it converges to a final solution.

After the last calibration is performed using Tracking Tools software, parameters are saved into a file to be used during tracking measurements.

Tracking tools let the user choose different calibration qualities before perform the acquisition using *Optiwand*. This parameter will modify the iterative process to be faster when a lower quality is selected. However it is

unknown how this parameter affects to the tracking error. Thus one important variable to be considered for the total error is the "Calibration Quality" parameter.

4.2   ROBOT CONNECTION

The robot is connected to the PC through an Ethernet service cable (see 3.3). The connection of the client with the robot server is performed creating two sockets in each system and using the communication protocol TCP/IP. This protocol ensures the correct transmission of data as it is a connection-oriented protocol, that is, it keeps track of the order and the size of the sent data, being reliable to know that the robot has received the data and that it returns the response to the client.

4.3   ROBOT PATH

Along all acquisitions a volume of 300x500x400 mm was swept with a point-to-point distance of 50 mm. This volume was centred inside the tracker field of view in order to simulate the patient tracked area. In order to avoid robot and tracker system collisions, the acquisition trajectory was tested in a previous simulation using RobotStudio into the robot (Figure 24). Tested trajectory was saved and employed for all the tracking data acquisition.
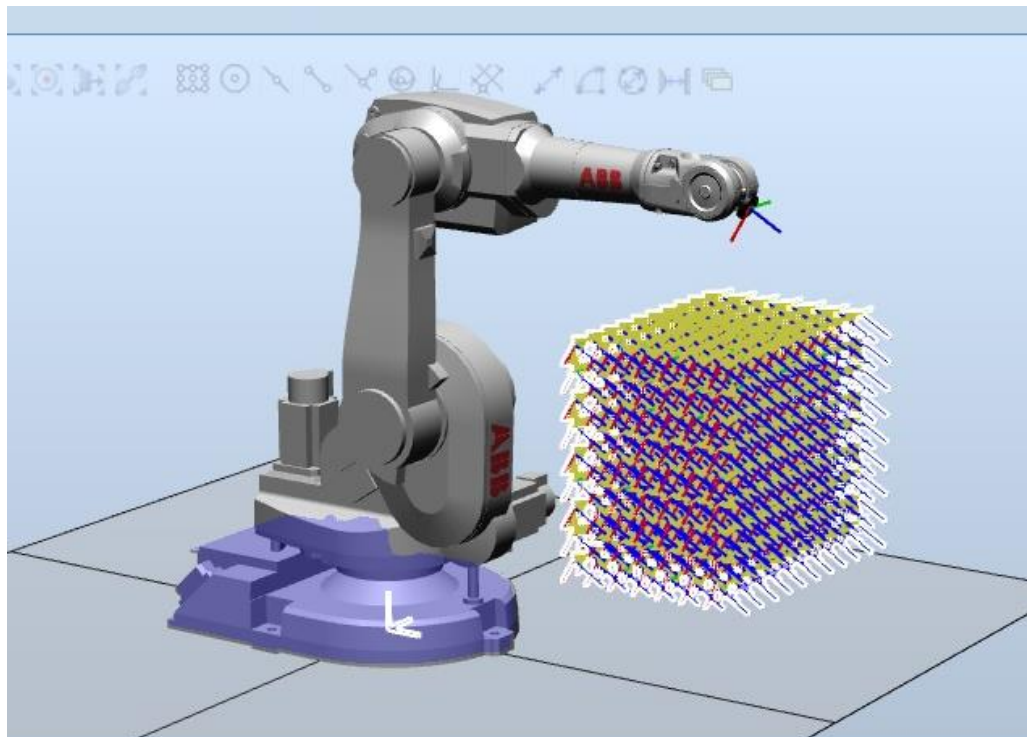
Figure 24
Robot path in RobotStudio. Same Matlab volume and points.

4.4   ACQUISITION WORKFLOW

The complete workflow for a single acquisition is depicted in Figure 26. First, the server is started in the FlexPendant. When it is ready to receive instructions and the robot is connected, the client runs in the computer. Socket connection is checked to work and once connection is established the client uses the Optitrack API and starts the tracking system. Client loads the specific files for calibration and tool definition and reads the trajectory file.

Next, first point localization is sent to the server that controls the robot and places the tool in the required position. Once the robot is correctly placed, it sends a signal back to the client that starts the tracking pose collection of the tool. At each single point, 1000 samples from the tracking system are collected following the employed protocol at HGGM.

Finally, the location data is appended to a '.txt' file, separated by commas (*csv* format compatible). The maximum number of points saved in one single file is 100 and the process is repeated until all the points in the trajectory are registered. Then the client closes the communication and ends.

4.5 ACQUISITIONS

The proposed experiments to test different camera setups and working conditions are summarized in Table 7.

Tracking one only marker

- **Number of occluded cameras study**
  - 8 cameras (none occluded, 10 repetitions)
  - 7 cameras (10 repetitions of 8 combinations occluding each camera)
  - 6 cameras (15 combinations occluding 2 random cameras)
  - 5 cameras (15 combinations occluding 3 random cameras)
  - 4 cameras (15 combinations occluding 4 random cameras)
  - 3 cameras (15 combinations occluding 5 random cameras)
- **Calibration quality study** (5 repetitions per experiment)
  - Low quality
  - Medium quality
  - High quality
  - Very High quality

Tracking rigid-body tool

- **Tools study** (10 repetitions per experiment)
  - Centroid of NDI Polaris
  - Pointer tip of NDI Polaris
  - Pointer tip of BiiG tool
  - Centroid of IOERT applicator tool
  - Centroid of rigid body (star-shaped) tool

Table 7
List of measurements.

First, a study about the cameras occlusion is performed. The total number of cameras was 8 with the aim of simulating the operating room set up. Using 8 cameras, 10 acquisitions of the complete trajectory were acquired. In order to study the accuracy of the tracking under occlusion conditions several trials were performed occluding different number of cameras (1, 2, 3, 4 and 5 occluded cameras). For each of these cases, 15 random combinations of cameras (with no repetition) were tested and

acquisition was carried out. In the case of 1 camera occluded (Table 7) all combinations were acquired (8 combinations).

For the 'Calibration Quality' Tracking Tools parameter study, three different calibrations were performed, each one with a different parameter selection: Low, Medium, High and Very High qualities. For each case 8 cameras were used and 5 acquisitions of the complete trajectory were carried out. In occlusion and in 'Calibration Quality' study a single marker was tracked to collect the system positions.

Finally, in order to study different tracked tools 5 trials were performed. Each tool was attached to the robot clamp and trajectory was acquired 5 times. The tools can be viewed in (Figure 23). Polaris Pointer accuracy was tested using both the tip position and the centroid of the tool. For the case of BiiG Pointer only the tip of the tool was used. The IOERT applicator also was tracked and finally a rigid body (star-shaped) provided by OptiTrack System that can be attached to any other tool of interest.

4.6   EVALUATION

The purpose of the evaluation is extracting quantitative measures of the tracking error and its mean value for every described setup. Due to the repeatability error of the robot (3.3), it is considered a gold standard compared to OptiTrack.

Usually, the error is measured as the difference between two localizations ([23]), that is, the ground truth and the evaluated position. However, during the experiments, the robot tracking information and OptiTrack positions are not given in the same 3D coordinate space. One possible approach could be to perform a registration between both point clouds. Nevertheless, the registration error is added to the final measure and the absolute tracking error of the system is masked. To overcome this limitation a specifically designed evaluation methodology was developed.

The main idea of the data evaluation is to extract the distance between localizations provided by OptiTrack and compare them with the actual one, which is 50 mm. The robot moves the tools with high accuracy and studied points are separated such fixed distance from each other. In order to get a single tracked position, at each point in the trajectory, the mean value of the 1000 samples is calculated. Then the distance of each point to the closest is extracted.

Each point has 6 neighbours and for each point six distance values are extracted. For points placed at the sides or corners, only the closest points are used so fewer values are extracted from these. At each point the

median is calculated from the set of extracted distances (m_i). Finally the Target Error (TE) at point p_i is computed as

$$TE(p_i) = \|m_i - g_t\|$$

where g_t is the ground truth distance (50 mm, Figure 25).
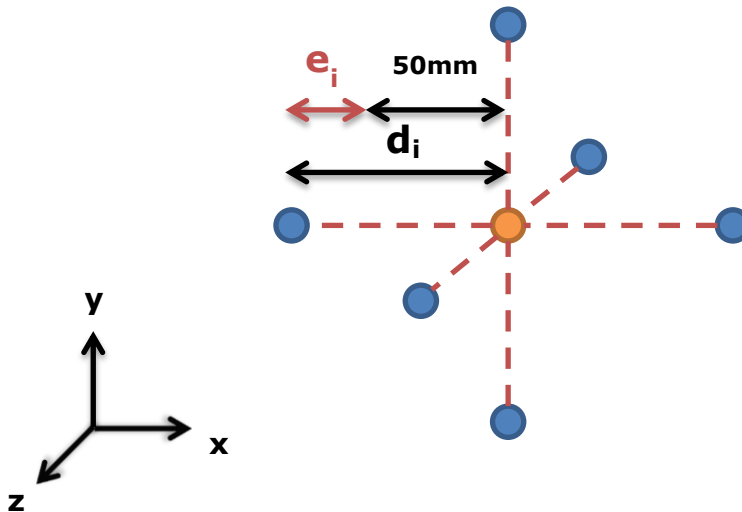
Figure 25
Six 3D mean neighbours (blue) around one mean point (orange).
The median of all distance errors (e_i) is the TE at point p_i.

In summary, for each acquisition a TE spatial map is extracted. As figures of interest the root mean square (RMS) value of TE for each trajectory point along repetitions will be extracted. Also, an RMS value along all repetition was extracted in each case.

5. RESULTS AND DISCUSSION

This section describes the results of this project. To start with, there is a brief description of the developed software. This software was specifically designed for the acquisition tasks and part of this project. Later, the quantitative results and discussion are presented along all acquisitions.

5.1   DEVELOPED SOFTWARE

The developed code includes the server that runs on the robot controller and a client that runs on Matlab. Both systems establish a connection and then the client will request the robot to move to consecutive points in order to track the position of a tool as was described before.
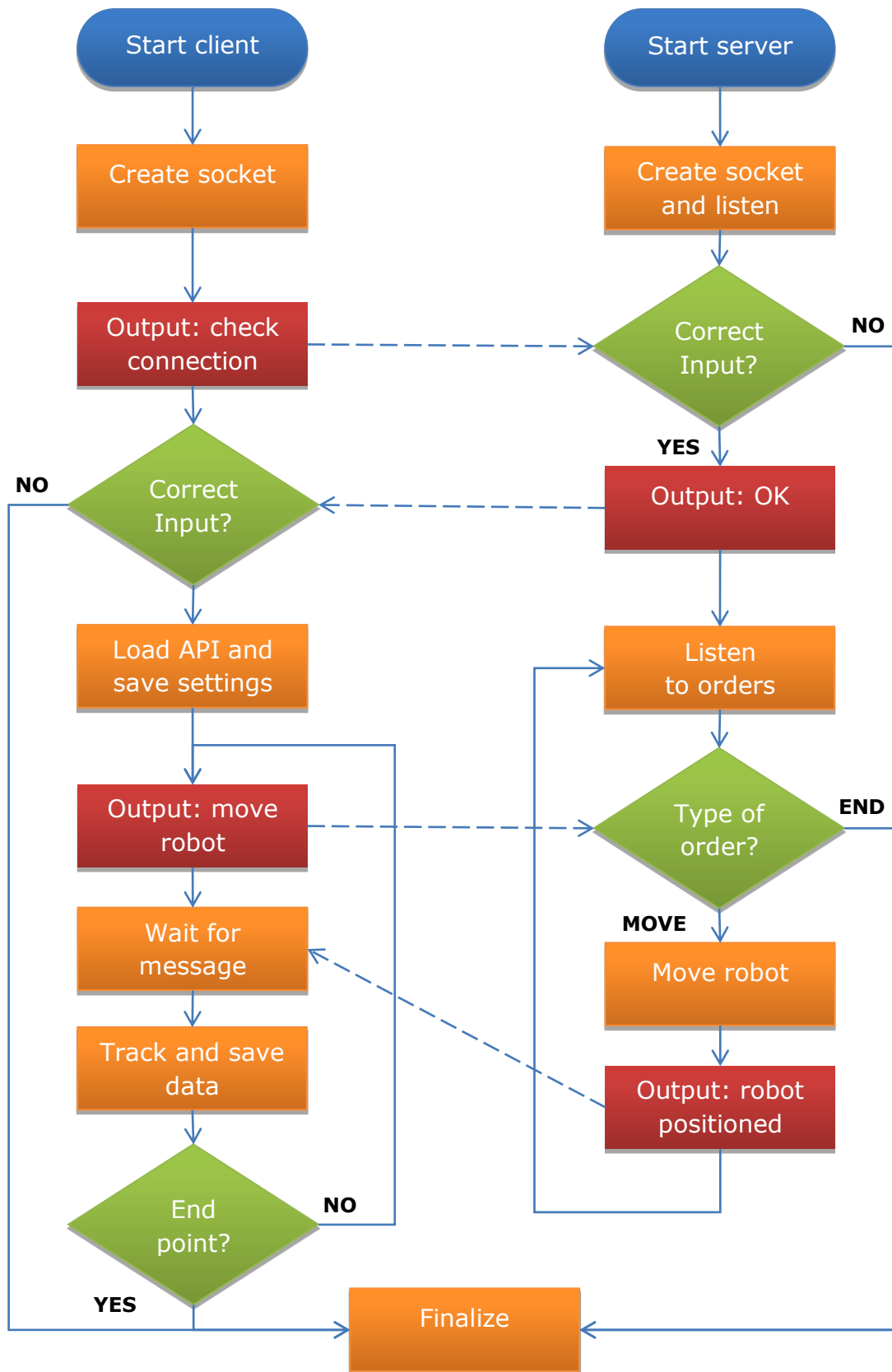
Figure 26
Flowchart of the client/server communication.

5.1.1 ROBOT SERVER APPLICATION

The RAPID server application has the task of listening to the client's requests. These include receiving the position data to move the robot. After moving the robot, it transmits a message back to the client for it to start tracking the position. This application have been based on two Bachelor Theses ([24], page 199; [25], page 119) from the UC3M.

The program follows three main steps; first, creating the connection with a TCP/IP socket to the client; secondly, checking the connection status; and finally, command listening.

This last step enters in a loop and can receive two different commands: one that commands the robot to move towards a certain position, and other that produces the closing the connection and finalizing the program. The server communicates with the client when it is ready to receive data. Then the positioning data is sent from the client to the server and robot is moved. Once the data is received, the robot moves and confirms this to the client, which will start tracking with OptiTrack.

After all the points have been tracked, the client will send the finalizing message to close the connection.

5.1.2 MATLAB CLIENT APPLICATION

The client task is to establish a successful connection with the robot server, request it to move to a new location and confirm when it is positioned to start tracking with the cameras. After the trajectory is completed, it sends a message to close the communication.

Two functions were developed to obtain the tracking information using Matlab and the Tracking Tools (Optitrack) API. One function was developed to track a rigid body centroid or pivot tool while another would track one passive marker only.

The processes for the data acquisition can be summarized as follows:

Declaration of variables	Robot connection	Ready API and tool	Move robot to position	Track with API	Save data
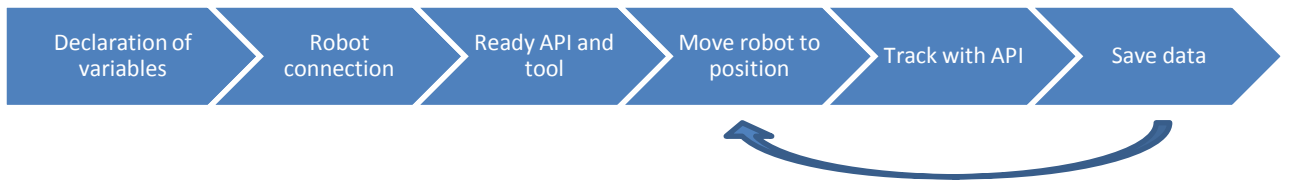
Table 8
Client application workflow.

The variables to configure include the calibration file, the number of samples taken by the cameras on the same point, the tool to be defined, the pivot of the tool selected, the number and position of the occluded cameras, the spatial step, the points of the path for the robot and the IP address and port to create a TCP socket.

The calibration file is the generated by Tracking Tools after the camera calibration. It is needed by the API to locate the camera positions and load the extrinsic and intrinsic parameters in order to be able to track.

The number of samples will determine how many location samples are taken per point. A tool parameter loads the specific tool selected. It will load the pivot and the tool markers' positions.

This configuration is saved in the same folder than the acquisition data in order to know the specific settings that were used in every measure and organize the data for the evaluation.

5.2   NUMBER OF OCCLUDED CAMERAS STUDY

The next figure shows the RMS (root mean squared) TE in millimetres by colouring a cube around each point. The colour scale indicates the RMS value of the error. The different results for several numbers of occluded cameras are depicted jointly.
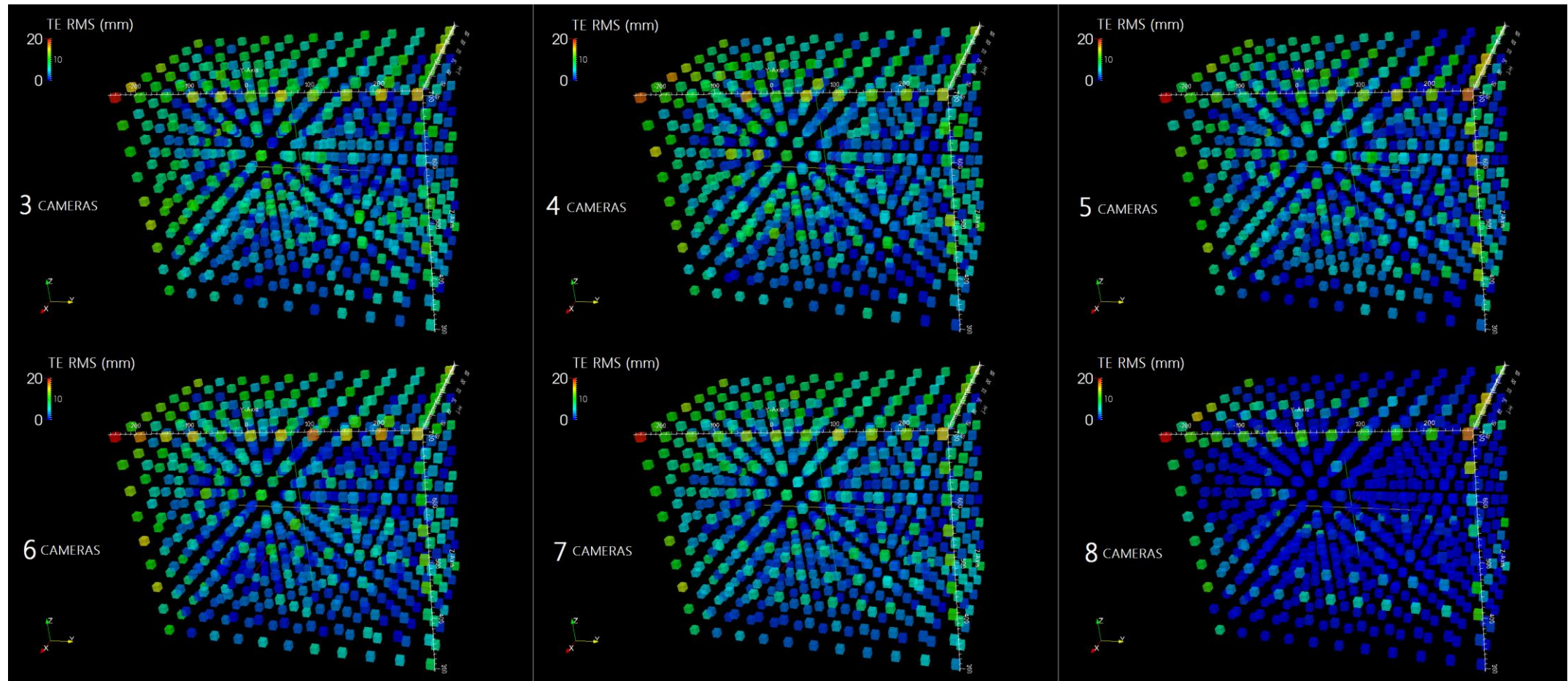
Figure 27
From left upper most to right lower: TE RMS (mm) for 3, 4, 5, 6, 7 and 8 cameras.

The following figure shows the TE distribution for different number of working cameras.
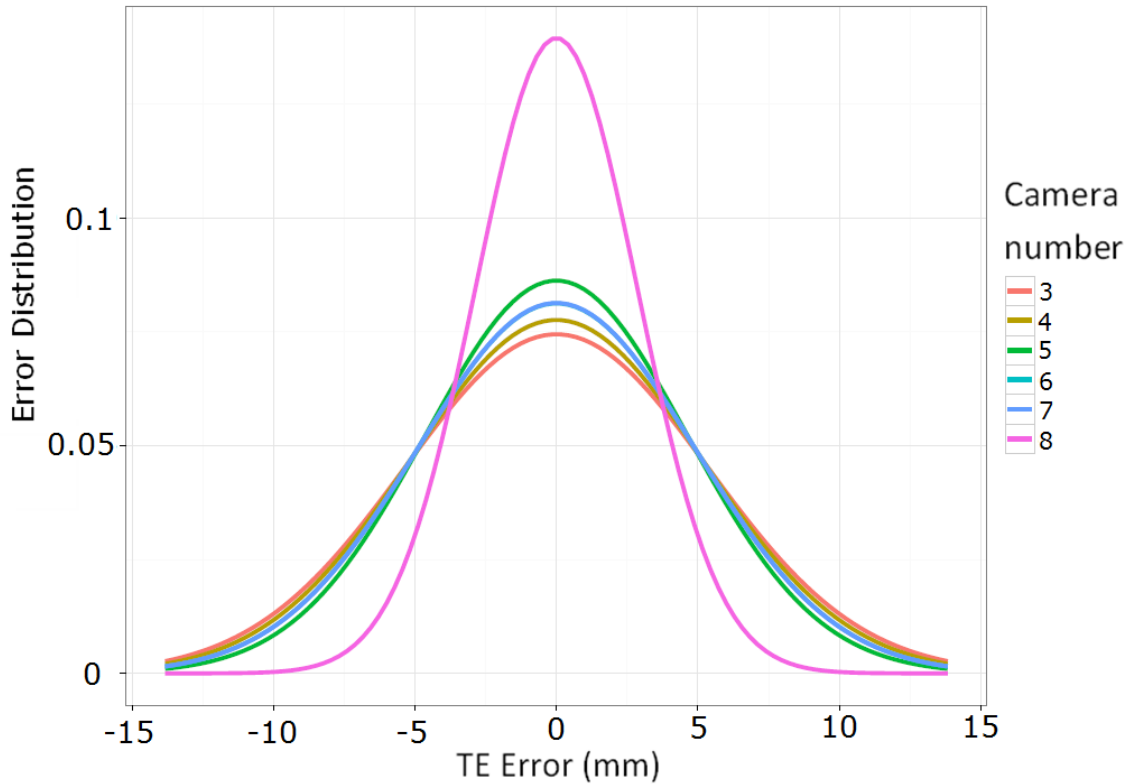
Figure 28
Error distribution for the occluded cameras study.

The next table shows the TE (RMS) along all studied points for each experiment. As we can see, TE decreases with the number of working cameras used during data acquisition.

Number of Occluded Cameras Study

Number of Working Cameras	TE RMS (mm)
3	5.36
4	5.14
5	4.63
6	4.91
7	4.91
8	2.86

Table 9
Results of the number of occluded cameras study.
TE RMS (mm).
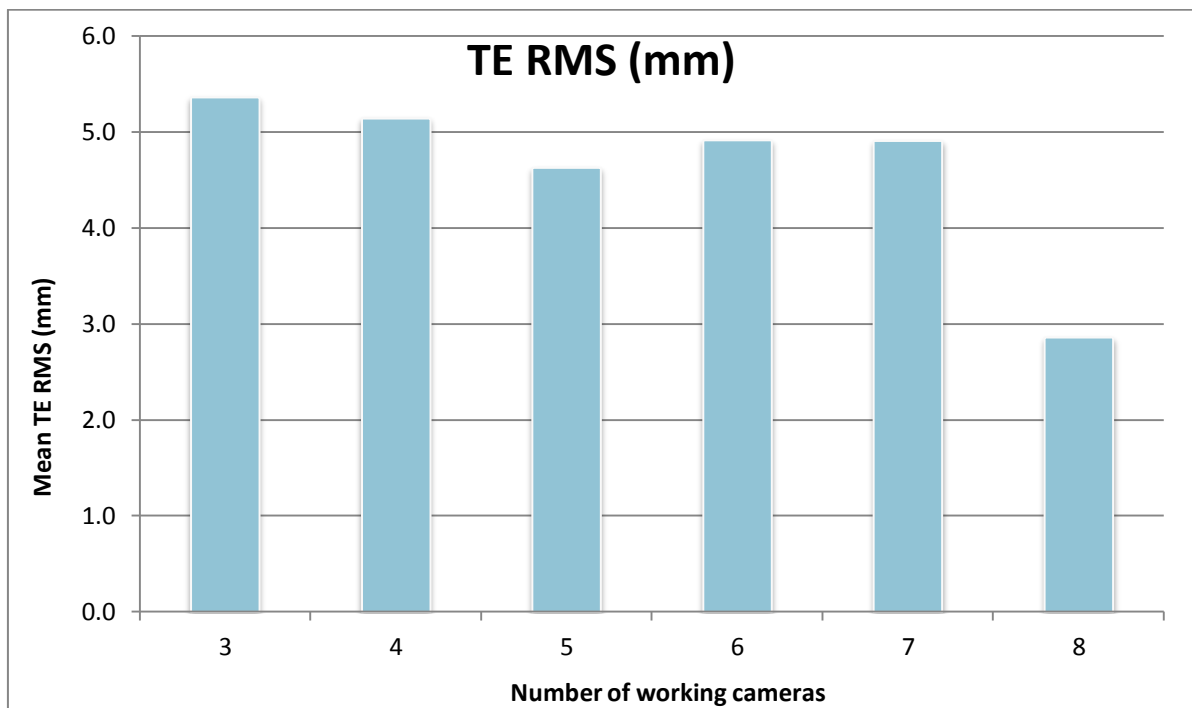
Figure 29
Graphical representation of the results for the number of occluded cameras study.
TE RMS (mm).
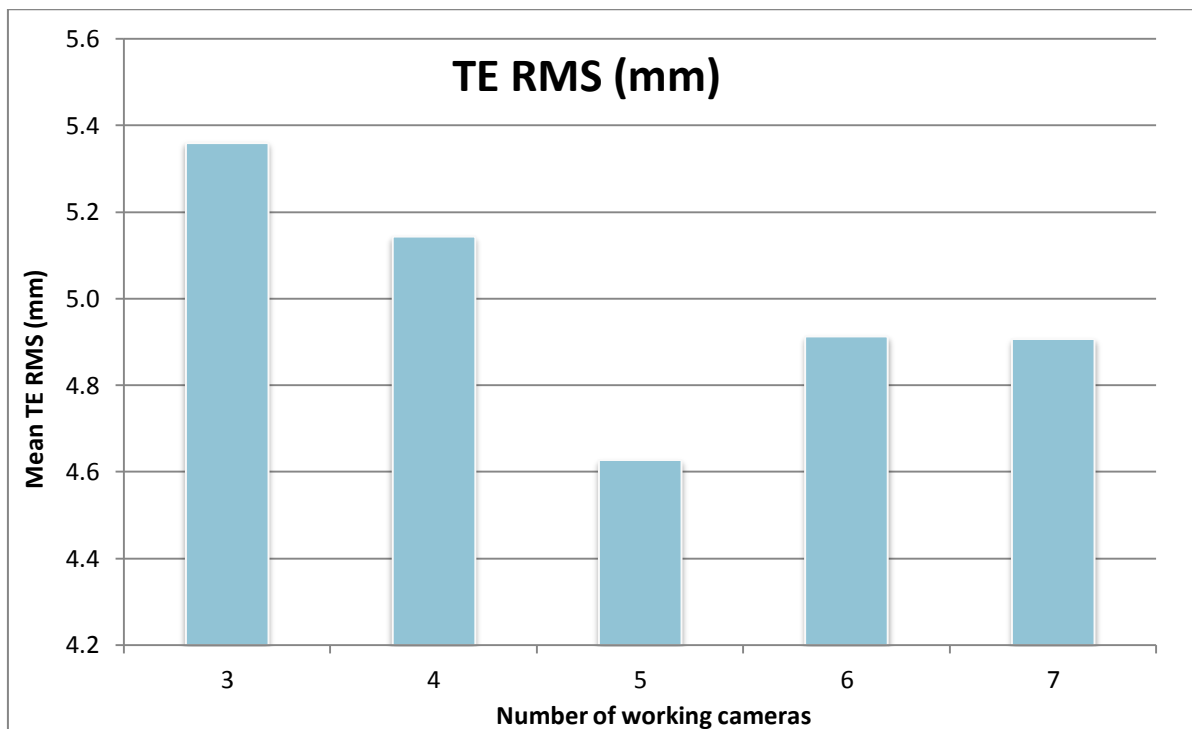
Figure 30
Graphical representation of the results for the number of occluded cameras study.
TE RMS (mm):
detail of differences between 3, 4, 5, 6 and 7 cameras.

The first figure (Figure 28) of this study represents the distribution of the error for the samples of every experiment. It can be seen that the best result is for the 8-cameras setup, where about 90% of the area under the curve (most of the samples) fall into a standard deviation of ±2.86 mm.

The other setups show worse similar results with its 90% into ±5 mm of standard deviation. The magnitudes of this deviation for every case are specified in Table 9.

The results in Figure 27 from this study not only show the error dependence on the number of occluded cameras but also shows the error depending on the spatial position.

The plot compares all camera setups in one picture. It can be seen that there is a lower error in the experiments performed with 8 cameras than with 4, 5, 6 and 7, that have come up with similar TE values. The measures with 3 cameras show also a considerable error increase compared to the others setups.

The graphics Table 9 and Figure 29 show quantitative data for the RMS error value depending on the number of working cameras.

In Figure 30 the small differences between 4, 5, 6 and 7 cameras setup can be appreciated. It shows that the deviation is smaller for 5 cameras than with 6 or 7. This can be due to unexpectedly good random combinations of working cameras. Several cameras are worse positioned than others, i.e. corner cameras. As occluded cameras were chosen randomly, there is a chance that the combinations were better for 5 cameras experiment than the 6 and 7 camera combinations.

Looking at Figure 29, the greatest deviation is found with 3 cameras (5.36mm), and the lowest with 8 cameras (2.86mm), being this difference of 1.2mm.

Regarding the spatial dependence of the error, in Figure 27 the TE is distributed in all cases with a higher error at the furthest points from the centre, that is, at the edges, than in the central points.

For example, in the TE for 8 cameras the spatial error difference is clearly appreciated: the TE is around 20mm (reddish colour) in the upper left and right corners, around 10mm (green colour) in the upper and left-most lines of points and it is close to zero in most central points where many cameras are focusing.

Notice that, on the one hand, the evaluation method depends on the neighbours, and at corners there are fewer neighbours so that the error appears higher.

But this tendency spreads also over points with 6 neighbours. This is consistent too because, on the other hand, the tool at corners is at the limit of the field of view of the cameras and not all the cameras have direct line of sight to the tool. Then it is expected that the error increases due to the lack of information. Inversely, the error at the centre points is considerably lower.

5.3   TOOLS STUDY

This study has analysed the TE for several different rigid-body tools (Figure 23, Table 7), in order to compare them. The configuration of the markers in 3D and the size of the markers, among other design characteristics, may make one tool better than another.
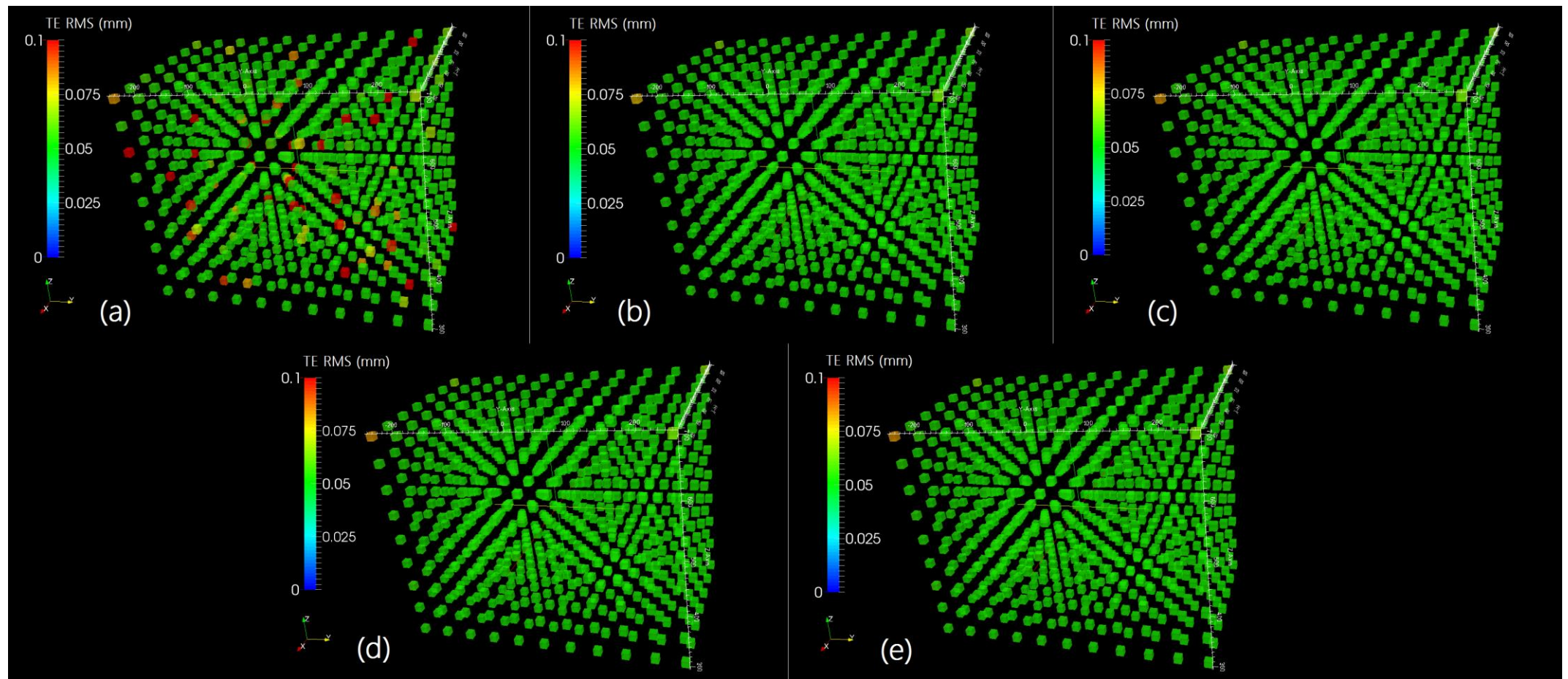
Figure 31
From upper left to lower right, TE RMS (mm) for each point with: BiiG tool tip (a), Polaris tool tip (b), Polaris tool centroid (c), rigid-body (star-shaped) tool centroid (d) and IOERT applicator tool centroid (e).

The tracked tools are, in the same order than their acquisition, as follows:
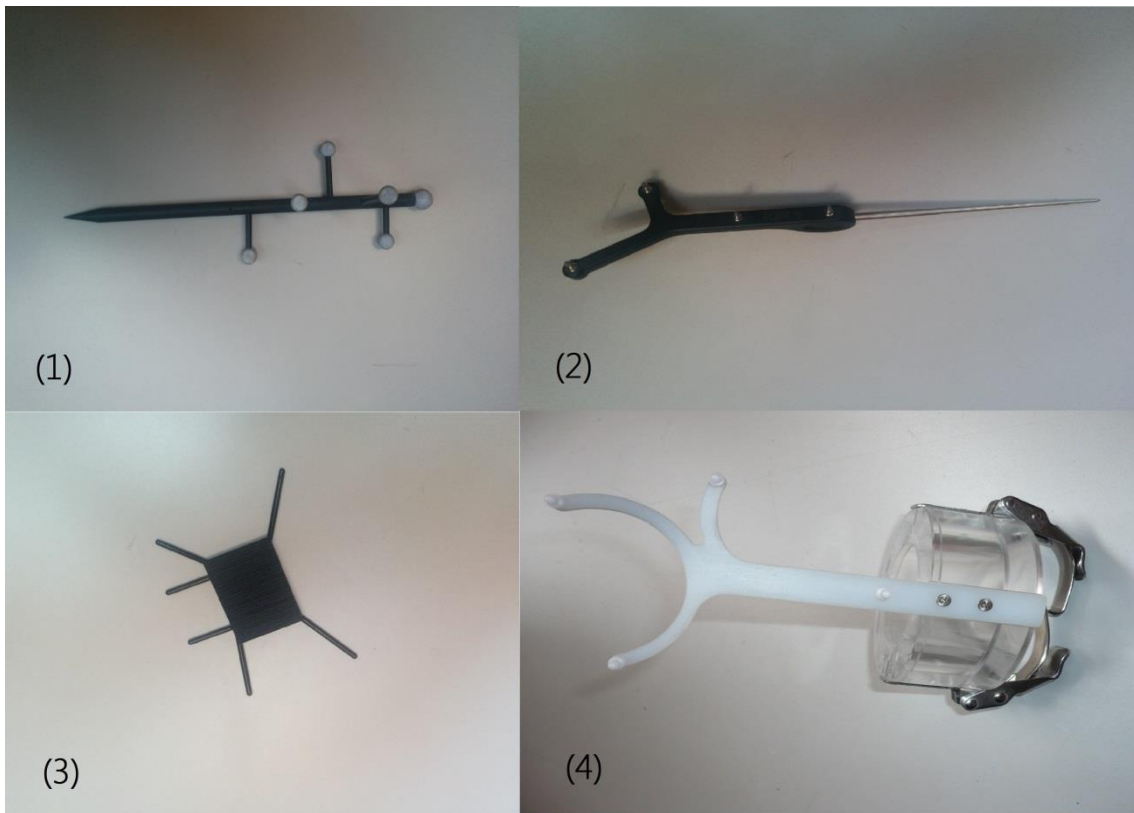
Figure 32
BiiG (1), Polaris (2), rigid-body (star-shaped) (3) and applicator tools (4).

As in the previous section, the error distribution is plotted for this study to see the standard deviation in each case.
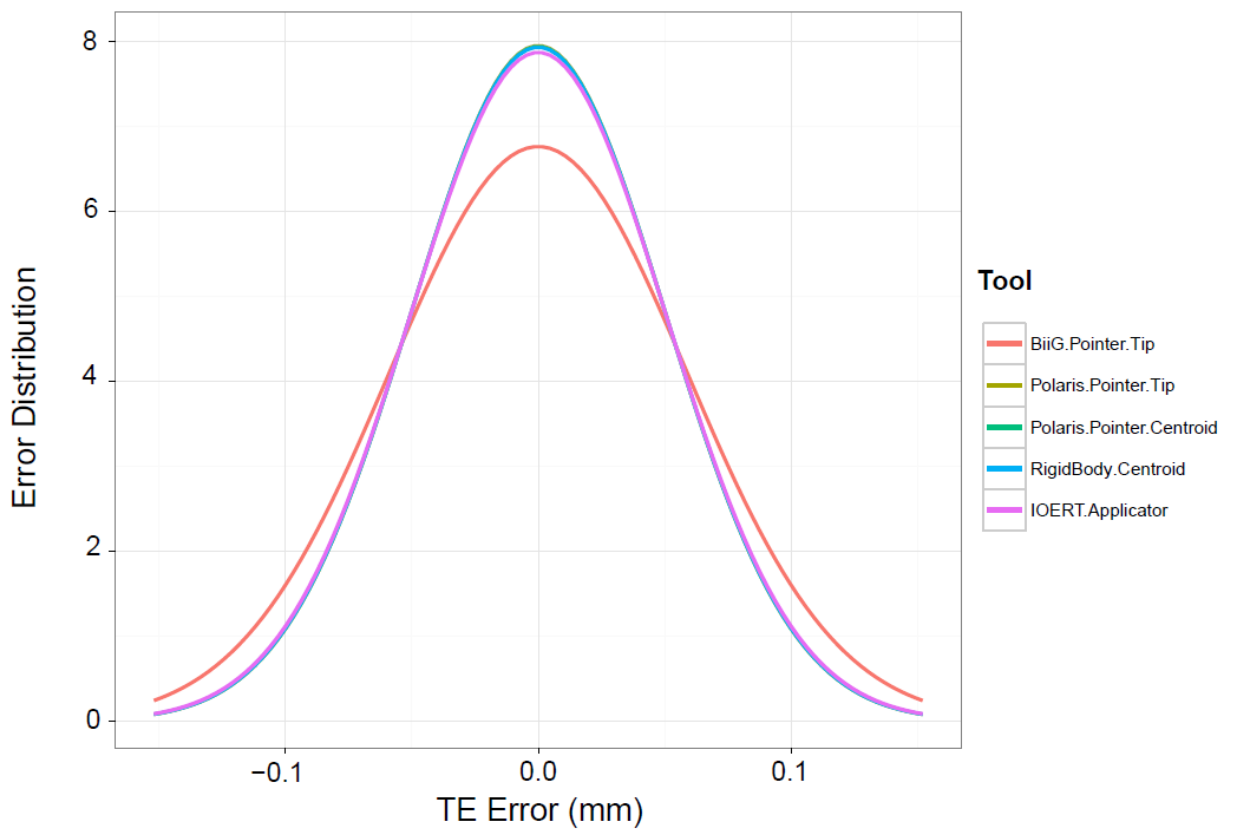
Figure 33
Error distribution for the tools study.

These measures are also calculated and shown in a graph to compare the values.

Tools Study

Tool	TE RMS (mm)
BiiG Pointer Tip	0.06
Polaris Pointer Tip	0.05
Polaris Pointer Centroid	0.05
RigidBody Centroid	0.05
IOERT Applicator	0.05

Table 10
Results of the tool study.
TE RMS (mm).
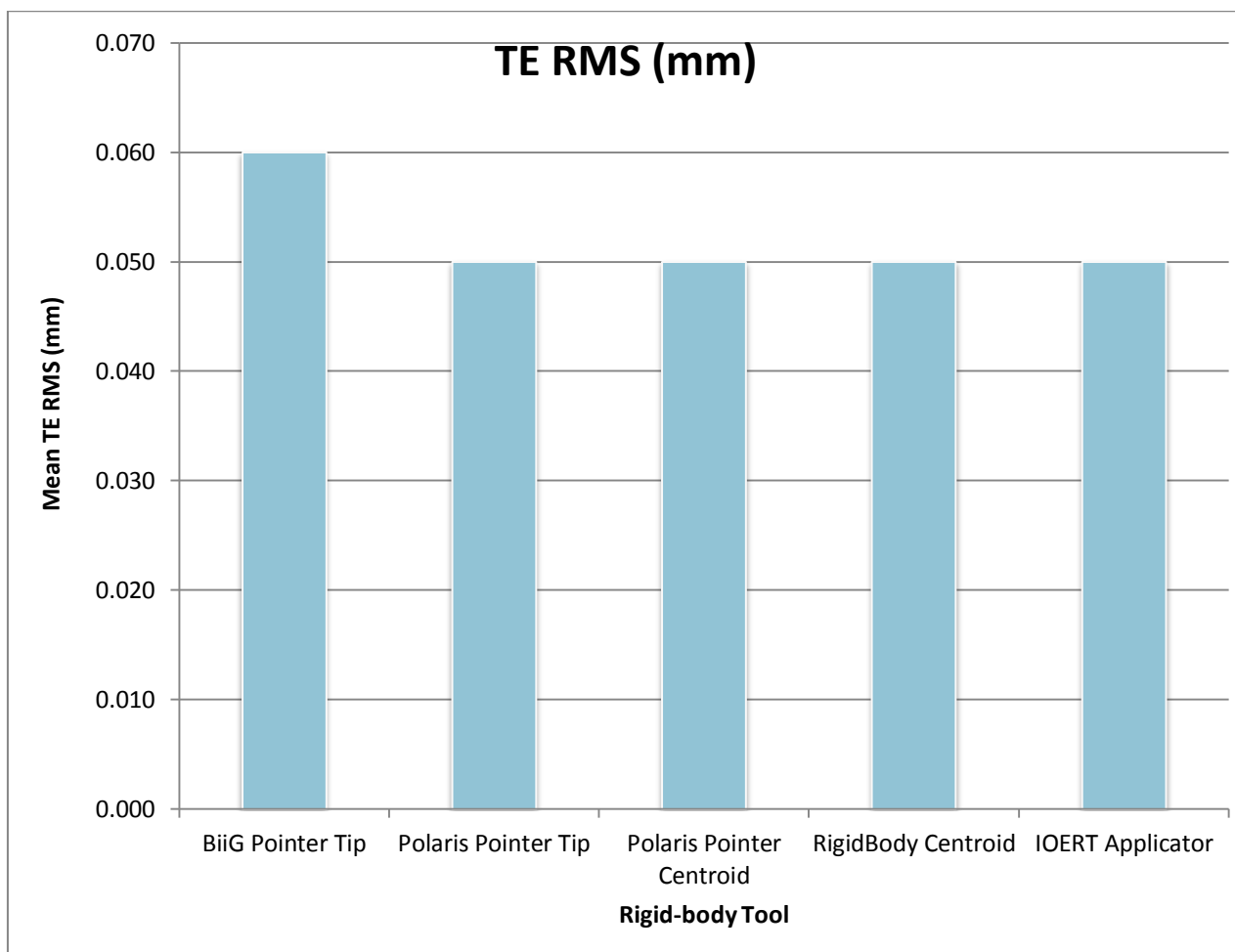
Figure 34
Graphical representation of the results for the tool study.
TE RMS (mm).

In the distribution of the error graph (Figure 33) it can be seen that the BiiG tool's 90% of the samples will have a higher deviation (±0.06 mm in Table 10) of standard deviation, while the other tools have all a little less (±0.05 mm).

The spatial dependence of the error also occurs in this study, though it is not so conspicuous. Remark that the positions in the occluded camera number study are from one only marker, while the tool study calculates it from all the markers. This method is useful to compare different tools, but it masks the specific error on each marker.

The fact that the error is much smaller in the tools study than in the occluded camera number study, despite the spatial difference, confirms that the position obtained from a least squared method of all markers' position gives better results than from one only marker ([23]). But apart from the

spatial positioning, there can be seen significant differences in TE between the BiiG-designed tool and the other tools. The maximum values on this tool reach 0.1 mm of TE on several points, while the others stay at 0.05 mm for all points except the furthest upper left corner, where they register around 0.8 mm.

The non distance-related character of the TE differences on the BiiG suggests the higher errors are caused by markers occluding other markers of the tool. This can be associated with this tool because it has the higher number of markers of all, and none of the rest shows these values and in those positions. Likewise, more markers mean they are more prone to occlude one of the other markers, and thus the positioning could fail.

This difference of the BiiG tool with the others is also reflected in the standard deviation. As Table 10 and Figure 34 show, the BiiG tool registers the highest value with 0.06 mm, while the best tool is the Polaris, with the pivot at the centroid: 0.05 mm. Note that the difference of 0.01 mm is in the range of the hundredth of a millimetre a value within the error of the robot. Excluding the BiiG tool, the rest show quite similar TE and deviation values.

5.4   CALIBRATION QUALITY STUDY

As in the previous studies, the TE and its rms has been calculated for different calibration qualities on Tracking Tools. Though there are many other configurable parameters, these calibrations differ only in the *Quality* selector tab available in the software to compare this setting's influence on the error.
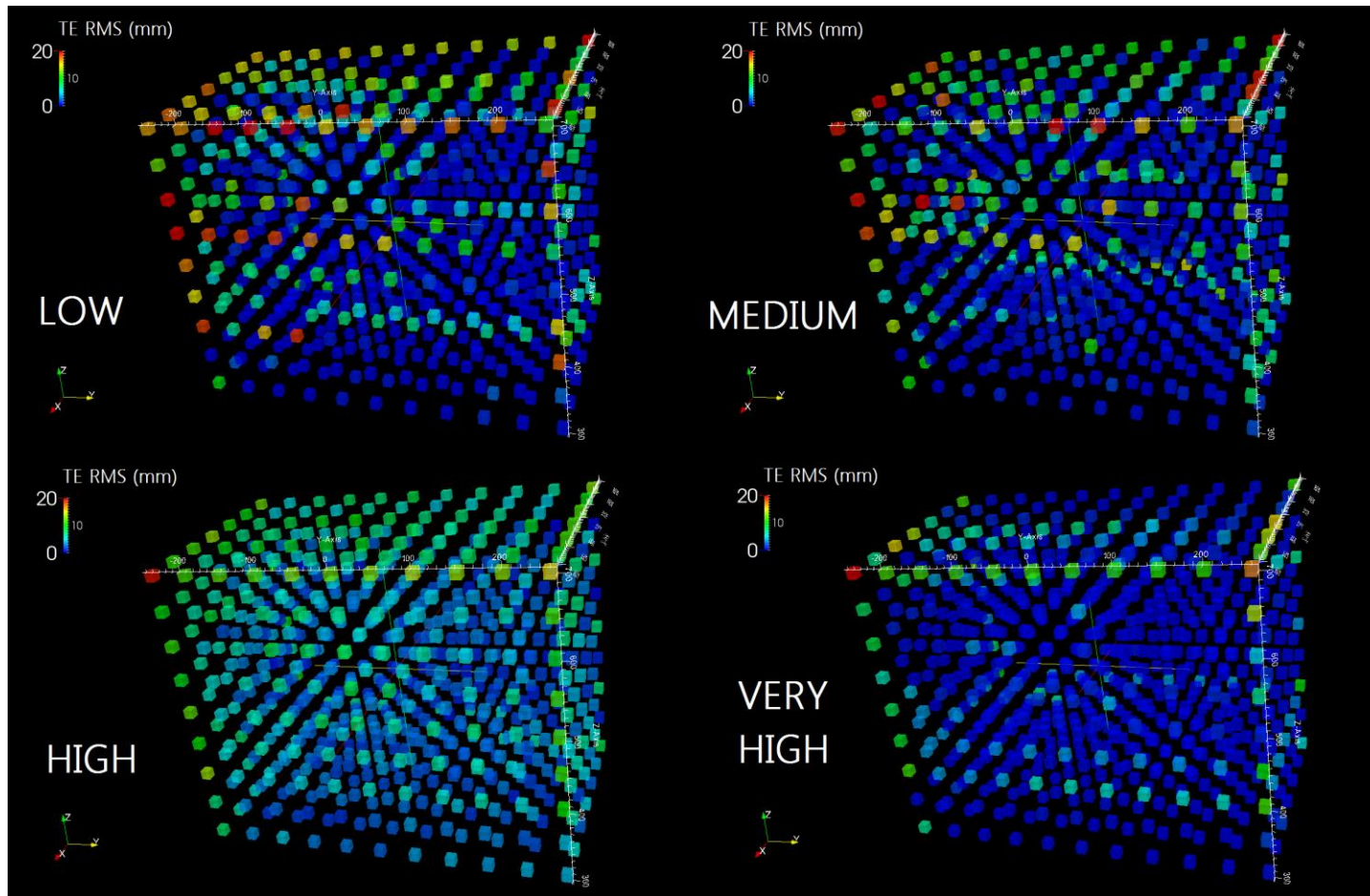
Figure 35
TE RMS (mm) for each point for: low quality (up left), medium quality (up right),
high quality (down left) and very high quality (down right) calibrations.

The error distribution of different calibration qualities is shown in the next graph:
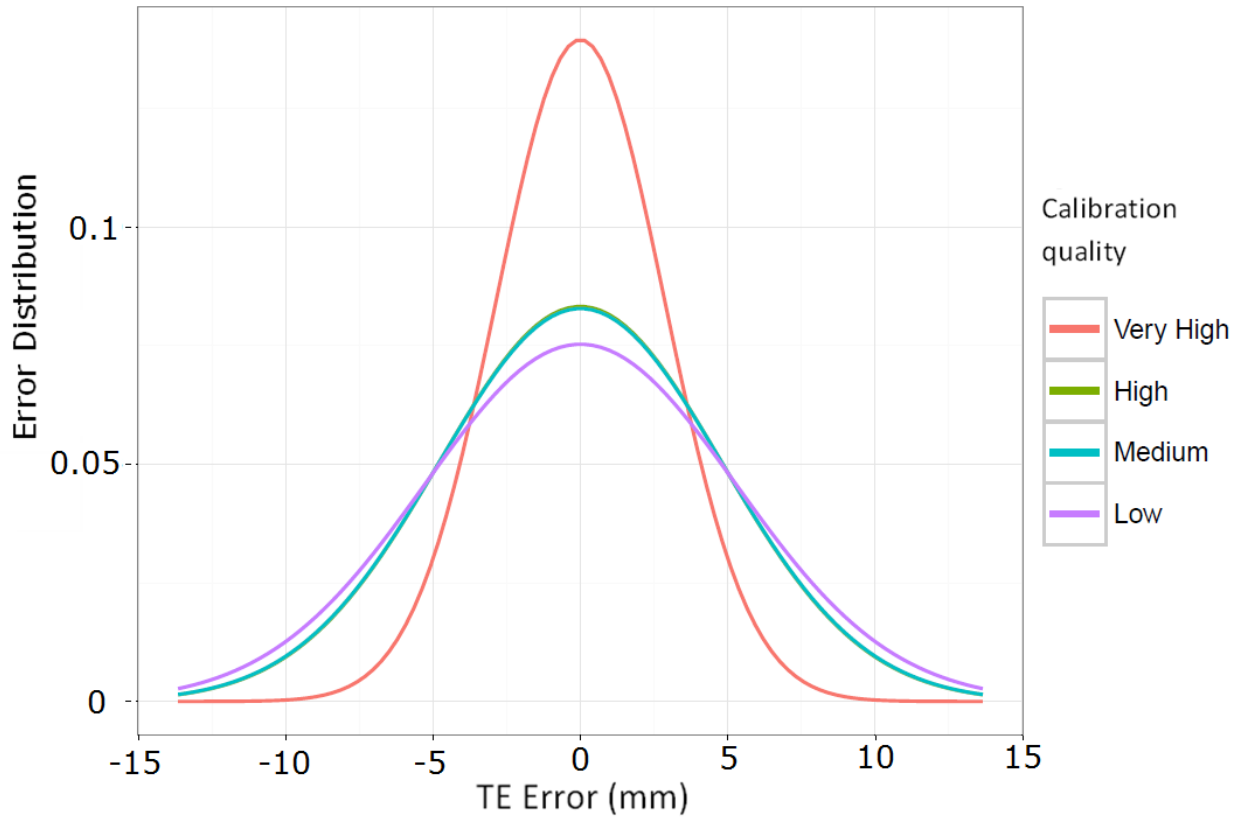
Figure 36
Error distribution for the calibration quality study.

Now the mean of these measures is calculated and shown for all the calibrations in a graph to compare them.

Calibration Quality Study

Calibration Quality	TE RMS (mm)
Very High*	2.86
High	4.79
Medium	4.82
Low	5.30

Table 11
Results of the calibration quality study.
TE RMS (mm).
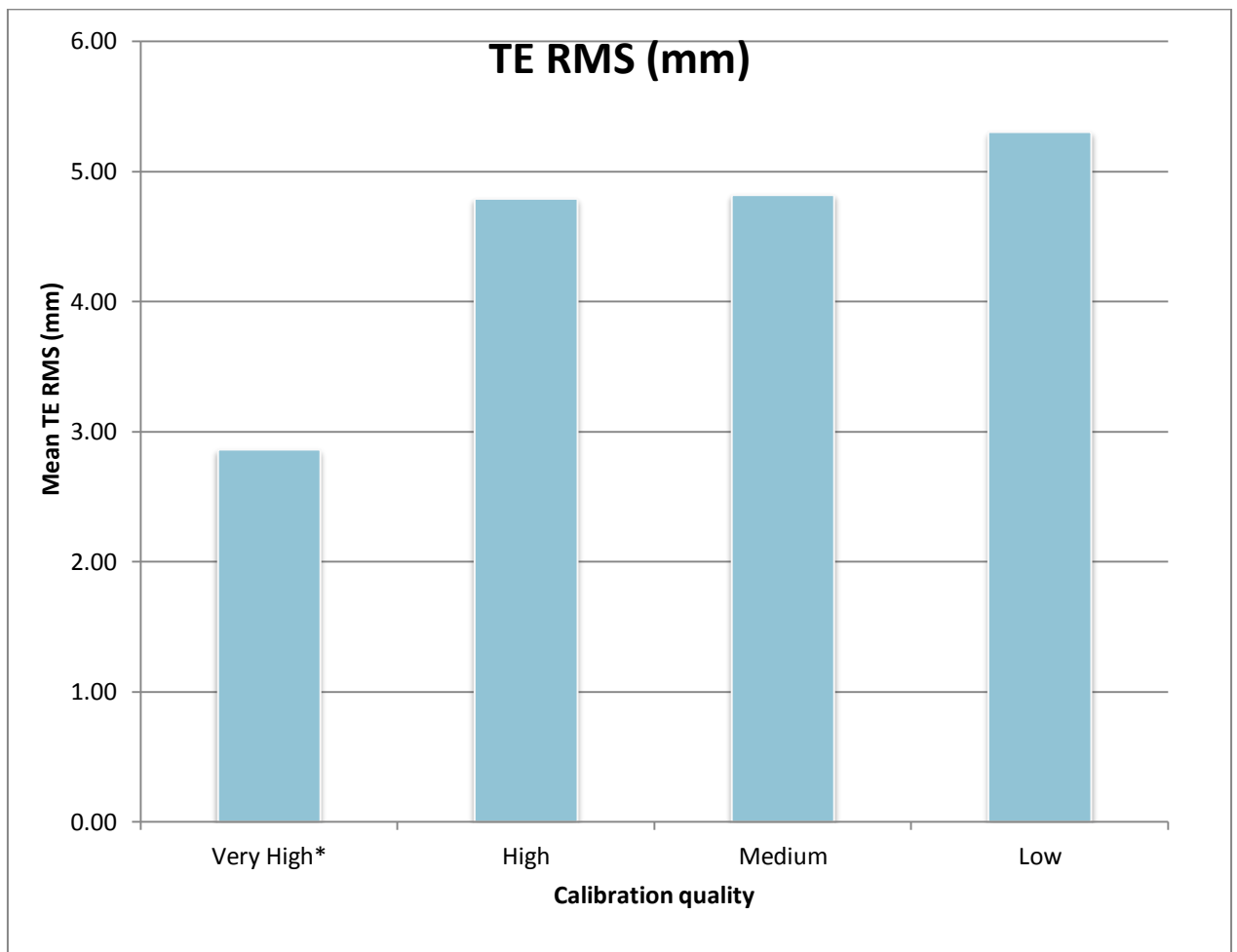
Figure 37
Graphical representation of the results for the calibration study.
TE RMS (mm).

Notice that there is one specific point in this study and in the previous ones that always shows a greater error: it is the point in the upper-left corner. This is probably due to a position in which the robot moves in the middle of the line-of-sight of several cameras.

The distribution of the error figure (Figure 36) shows the best results for the very high quality calibration, as expected. Its 90% of samples have ±2.86 mm of standard deviation. The medium and high qualities show both an standard deviation of about ±4.8 mm, while it goes up to ±5.30 mm in the case of low quality.

In this study, the figures show clear differences between the three calibration qualities. The first image corresponds to the low quality calibration acquisition. Quite a few points have a remarkably higher error than the others two calibrations. Thus, the error is higher and on a larger volume with the low calibration.

The second picture, which corresponds to the medium quality results, shows also several points affected by a higher error, though in not so many points than the low quality.

In the last image the differences can be easily assessed. It shows clearly less error magnitude and on almost all the volume covered. This corresponds to the high quality calibration.

Finally, the very-high quality shows the best results of all; this measure was obtained making a pre-calibration first and selecting additional parameters in the same way as it is done in the OR.

The results on position error are consistent with the expected behaviour of the software Tracking Tools when calibrating. Analysing the standard deviation values (Table 11 and Figure 37), it can be confirmed the differences between the qualities of the calibrations, though the medium and high qualities show little difference (0.03 mm), while there is clearly a higher error in the low quality (0.51 mm). Also, the very-high quality shows the greatest difference with the low quality (2.44 mm) confirming that the calibration stage is important on the final error.

As mentioned before, this study takes into account only the general quality distinction of the software, but many other parameters of the calibration are available to configure. As these are user-selected, the study has centred on analysing the main quality differences.

6. CONCLUSION

The tests performed in these experiments with OptiTrack have determined the spatial accuracy of the setup at the HGGM with different number of working cameras. It has also served to compare several tools with different designs, as well as the differences between selecting several calibration qualities.

Moreover, the developed software that controls the systems to make the acquisition possible can be useful to evaluate other configurations and behaviours of the OptiTrack system.

With this information, the IOERT navigation in HGGM has now a research study that backs up the use of OptiTrack tracking system and gives an estimation of the accuracy in real-life scenarios, also reasserting this system's use for medical applications.

Nevertheless, the OptiTrack system is very flexible, i.e. it can work with up to ninety-six cameras and they can be placed with many other configurations. This means that there are other factors to take into account in order to know the precision of a specific tracking configuration. These include the field of view of the cameras, the focused area and the cameras spatial distribution.

Additionally, it has been remarked in the number of occluded cameras study that more repetitions of the experiments should be made to have a better estimation; without time limitation, the more experiments, the more statistics are obtained which yields better distributed data.

Also, in the tools study it has been mentioned that the higher number of markers on a tool makes it easier for them to occlude among themselves, thus worsening the acquisition.

It has also been noted the difference in error between tracking a single marker and tracking the position of a rigid body, which is about two orders of magnitude better for the rigid body. This suggests that Tracking Tools is optimized for tracking rigid bodies as expected.

Regarding the calibration, though the error is known, it would be interesting to establish a method that ensures repeatability, as well as study several factors, like the wand used, the covered area with the wand, the parameters of the calculations and the pre-calibration steps.

Regarding the usage of OptiTrack system, the conclusions from this study are:

- It has been proven that the more cameras, the less error, as it is reasonable. More cameras means there is a higher chance all the rigid-body markers are seen in one frame by a high number of cameras, and thus a good positioning is more probable.

- The calibration is an important factor in the final error estimation. Without considering other parameters, at least a 'Medium' or 'High' quality should be selected in Tracking Tools. These two showed similar low errors, in contrast to a higher error in the 'Low' quality.

- The rigid-body tools are the best option for positioning because they are stable and they minimize the possible errors on single markers.

- Although a specific study to the design of tools is needed, it can be stated that the tools should have a moderate number of markers to avoid occlusions among them.

Finally, this study will serve as a guide to improve the tracking results for any user or application that uses this system, but the ultimate utility of this study would be to help the physician at the time of an image-assisted IOERT procedure. For that, the error given by a camera setup and the different factors that affect it can be fitted to the results obtained and shown in real-time on the navigation.

7. FUTURE WORK

As commented, the effect of occluded cameras in some experiments requires more repetitions to improve the statistics obtained.

The study of the tools also demands a deeper study considering the effect of the optimum number of markers, the different marker sizes and the geometry.

To have a complete knowledge and characterization of the behaviour of OptiTrack system in any configuration it is needed to study the error dependence on these additional factors:

- Camera:
    - Camera model and characteristics
    - Camera spatial distribution
    - Camera focused area

- Calibration
    - Pre-calibration steps
    - Calibration parameters
    - Type of wanding tool
    - Covered area during calibration

However, for most applications the main factors are the ones tested in this study and the results obtained are in accordance to the requirements of medical purposes.

Lastly, the immediate application regarding this project is to aid the IOERT experts during the procedure by means of displaying the estimated error of the tracking system in real-time. To do this, the obtained data should be integrated with *radiance*.

8. BIBLIOGRAPHY

[1]   V. García-Vázquez, E. Marinetto, J. A. Santos-Miranda, F. A. Calvo, A. Camacho-Márquez, M. Desco, and J. Pascau, "Estudio de la Viabilidad de la Integración de un Sistema de Posicionamiento Óptico en el Entorno de la Radioterapia Intraoperatoria," in *XXIX Annual Congress of Spanish Biomedical Engineering Society (CASEIB 2011)*, 2011.

[2]   K. Cleary and T. M. Peters, "Image-guided interventions: technology review and clinical applications.," *Annu. Rev. Biomed. Eng.*, vol. 12, pp. 119–42, Aug. 2010.

[3]   F. A. Calvo, R. M. Meirino, and R. Orecchia, "Intraoperative radiation therapy first part: rationale and techniques.," *Crit. Rev. Oncol. Hematol.*, vol. 59, no. 2, pp. 106–15, Aug. 2006.

[4]   J. A. Torok, M. Palta, B. G. Czito, and C. G. Willett, "Intraoperative radiation therapy in the treatment of gastrointestinal malignancies," pp. 5–8, 2014.

[5]   GMV, "Radiation Treatment Planning System For IORT - Short Product Description," no. May. pp. 1–13, 2012.

[6]   J. Pascau, J. A. Santos Miranda, F. A. Calvo, A. Bouché, V. Morillo, C. González-San Segundo, C. Ferrer, J. López Tarjuelo, and M. Desco, "An innovative tool for intraoperative electron beam radiotherapy simulation and planning: description and initial evaluation by radiation oncologists.," *Int. J. Radiat. Oncol. Biol. Phys.*, vol. 83, no. 2, pp. e287–95, Jun. 2012.

[7]   E. Marinetto, V. García, J. A. Santos, F. A. Calvo, M. Desco, and J. Pascau, "Integrating optical tracking into IOERT workflow," 2010.

[8]   R. M. Martínez Mañas and E. Ferrer Rodríguez, "Precisión y utilidad de la neuronavegación en la cirugía encefálica," Universidad de Barcelona.

[9]   F. Calvo, C. Sole, R. Herranz, M. Lopez-Bote, J. Pascau, A. Santos, A. Muñoz-Calero, C. Ferrer, and J. Garcia-Sabrido, "Intraoperative radiotherapy with electrons: fundamentals, results, and innovation.," *Ecancermedicalscience*, vol. 7, p. 339, Jan. 2013.

[10]   T. Peters and K. Cleary, *Image-Guided Interventions*. 2008, p. 576.

[11]   The Online Medical Devices Exhibition, "Medical Expo - Stereotactic frame." [Online]. Available: http://www.medicalexpo.com/medical-manufacturer/stereotactic-frame-1219.html.

[12] V. García-Vázquez, E. Marinetto, J. a Santos-Miranda, F. a Calvo, M. Desco, and J. Pascau, "Feasibility of integrating a multi-camera optical tracking system in intra-operative electron radiation therapy scenarios.," *Phys. Med. Biol.*, vol. 58, no. 24, pp. 8769–82, Dec. 2013.

[13] OptiTrack, "OptiTrack - Flex 13 Camera." [Online]. Available: https://www.naturalpoint.com/optitrack/products/flex-13/.

[14] R. Hartley and A. Zisserman, "Multiple View Geometry in Computer Vision," *Robotica*, vol. 23, no. 2, pp. 271–271, Mar. 2005.

[15] R. Gooch, "Optical metrology in manufacturing automation," *Sens. Rev.*, vol. 18, no. 2, pp. 81–87, 1998.

[16] NDI, "NDI Polaris Optical Tracking System." [Online]. Available: http://www.ndigital.com/medical/products/polaris-family/.

[17] J. M. Fitzpatrick, "The role of registration in accurate surgical guidance," *Proc. Inst. Mech. Eng. Part H J. Eng. Med.*, vol. 224, no. 5, pp. 607–622, May 2010.

[18] ABB, "ABB IRB 1600 brochure." [Online]. Available: http://www05.abb.com/global/scot/scot241.nsf/veritydisplay/3b0491a94bd700a248257c71004ef393/$file/PR10282EN_R8.pdf.

[19] NaturalPoint, "Motion Capture Systems - Optitrack." .

[20] Global Robots Ltd, "ABB IRB 1600 Industrial Robot with M2004 IRC5 controller." .

[21] "BBC News - BUSINESS - Robot investment on the rise." [Online]. Available: http://news.bbc.co.uk/2/hi/business/1629753.stm.

[22] Naturalpoint, "Tracking Tools - Technical Specifications." [Online]. Available: https://www.naturalpoint.com/optitrack/products/tracking-tools/specs.html.

[23] J. M. Fitzpatrick and J. B. West, "The distribution of target registration error in rigid-body point-based registration.," *IEEE Trans. Med. Imaging*, vol. 20, no. 9, pp. 917–27, Sep. 2001.

[24] R. Bogdan and S. Martínez de la Casa, "SENSOR DE FUERZA PAR EN UN ROBOT ABB IRB 1600 (II)," UC3M, 2012.

[25] M. Á. Yunta and S. Martínez de la Casa, "Implementación de las comunicaciones pc-autómata-robot mediante interfaz ethernet industrial," UC3M, 2010.

9. APPENDIX

9.1 GLOSSARY

3D: Three dimensions

API: Application Programming Interface

BiiG: Biomedical Imaging and Instrumentation Group

EBRT: External Beam Radiation Therapy

HDR: High-Dose Rate

HGGM: Hospital General Gregorio Marañón

IGS: Image-Guided Surgery

IORT: Intra-Operative Radiation Therapy

IOERT: Intra Operative Electron Radiation Therapy

IR: Infrared

LED: Light Emitting Diode

MS: Microsoft

NDI: Northern Digital Inc.

OR: Operating Room

PC: Personal Computer

RMS: Root mean square

SDK: Software Development Kit

TE: Target error

UC3M: Universidad Carlos III de Madrid

USB: Universal Serial Bus

VS: Visual Studio

9.2 LIST OF FIGURES

9.3   LIST OF TABLES